
Article:
Gordon, L.E., San Nicolas, R. and Provis, J.L. (2014) Chemical characterisation of metakaolin and fly ash based geopolymers during exposure to solvents used in carbon capture. International Journal of Greenhouse Gas Control , 27. pp. 255-266. ISSN: 1750-5836

https://doi.org/10.1016/j.ijggc.2014.06.005

This is a pre-print of a paper published in *International Journal of Greenhouse Gas Control*, http://www.sciencedirect.com/science/article/pii/S1750583614001625.
Please cite this paper as: Gordon, L.E.; San Nicolas, R.; Provis, J.L. "Chemical characterisation of metakaolin and fly ash based geopolymers during exposure to solvents used in carbon capture," *International Journal of Greenhouse Gas Control,* **2014,** *27*: 255-266. DOI 10.1016/j.ijggc.2014.06.005

Chemical characterisation of metakaolin and fly ash based geopolymers during exposure to solvents used in carbon capture

Laura E. Gordon[a,b], Rackel San Nicolas[a,b], John L. Provis[a,b,c]*

[a]*CO2CRC, University of Melbourne, Victoria 3010, Australia*
[b]*Department of Chemical & Biomolecular Engineering, University of Melbourne, Victoria 3010, Australia*
[c]*Department of Materials Science and Engineering, University of Sheffield, Sheffield, S1 3JD, South Yorkshire, UK*

** Corresponding author. Tel.: +44 (0)114-222-5490; fax:+44 (0) 114-222-5943. E-mail address:j.provis@sheffield.ac.uk.*

Abstract

This paper presents an investigation into the chemical resistance of blended alkali activated aluminosilicate materials, specifically under exposure to two solvents used in post-combustion carbon capture, monoethanolamine (MEA) and potassium carbonate, as well as during immersion in distilled water. Geopolymers are formulated based on metakaolin and on fly ash as aluminosilicate precursors, with the addition of ground granulated blast furnace slag (GGBFS) as a source of Ca. The samples are subjected to mineralogical and chemical characterisation in this paper, with data obtained through leaching analysis and X-ray diffraction, supported by compressive strength data. Exposure to solvents generally results in significant alteration of the geopolymer microstructure. The zeolitic phases formed in undamaged metakaolin-based binders are reduced to undetectable levels after 28 days of solvent exposure, although the hydrosodalite formed in the fly ash binders does persist. Leaching analysis indicates that resistance to structural damage in MEA is quite high, due to the low solubility of Na and hydroxides upon immersion. K_2CO_3 solutions are aggressive towards geopolymers via alteration of the binder structure and dissolution of network-forming species (Si and Al), leading to the loss of binder strength. This is most marked in the fly ash/GGBFS formulations. Despite the low to intermediate level of Ca present in these geopolymer binders, significant formation of Ca-containing carbonate phases occurs upon

exposure to K_2CO_3. The limited curing duration of the specimens tested here is certainly contributing to the degradation taking place under K_2CO_3 exposure, whereas the low water activity in the MEA solutions used means that bond hydrolysis in the aluminosilicate geopolymer framework is restricted, and the materials perform much better than in a more water-rich environment.

Keywords: Construction materials; process equipment; concrete; geopolymer; solvent processes

1. Introduction

Traditional cementing binders are formed via the hydration reactions of calcium silicate phases, whereas geopolymer concretes are synthesised by the alkali activation of aluminosilicates to form the binder. There is currently widespread research into the development of geopolymers and alkali activated systems (Provis 2014; Provis and van Deventer 2014), motivated not only by the beneficial technical properties of the material, such as thermal and chemical resistance, but also by the greatly reduced carbon emissions in geopolymer production relative to traditional cementing binders (McLellan et al. 2012). It is estimated that 5-8% of global anthropogenic carbon emissions are due to cement production (Olivier et al. 2012), driving research towards forming alternative low emissions binders as a viable commercial option (van Deventer et al. 2010; Juenger et al. 2011; van Deventer et al. 2012).

As a means of reducing the CO_2 emissions profiles of the global energy and cement industries, which are large point sources of CO_2, carbon capture and storage (CCS) processes and facilities are currently being trialed (Jenkins et al. 2012), with viability depending strongly on the costs involved. Post-combustion carbon capture solvent columns are generally constructed from stainless steel, as good mechanical performance and a high degree of chemical resistance are required from a column construction material. Geopolymer concretes are proposed to provide a durable, cost saving 'green cement' alternative structural material for the construction of large CCS facilities, with the aluminosilicate geopolymer chemistry suggested to provide the possibility of withstanding the harsh chemical environments found within these systems (Gordon et al. 2011) as the chemical resistance of geopolymers has long been promoted as a benefit of these materials (Davidovits 1991), and has been highlighted in laboratory testing over a number of years (Davidovits 1991; Bakharev 2005; Fernández-Jiménez et al. 2006; Duxson et al. 2007a; Sindhunata et al. 2008; Fernández-Jiménez and Palomo 2009; Temuujin et al. 2011).

There are many appealing aspects of geopolymer concretes which may make them suitable for use as a construction material in carbon capture facilities. Relative to traditional concreting systems based on ordinary Portland cement (OPC), geopolymers can offer as much as 80% reduction in CO_2 emissions (Duxson et al. 2007b) These materials also utilise industrial wastes such as fly ash as an integral binder component; fly ash is currently landfilled at a rate of several million tonnes p.a. in Australia alone, and hundreds of millions of tonnes p.a. worldwide, bringing appealing synergies if the material was to be used in carbon capture applications associated with coal-fired electricity generation.

77 Fly ash is a by-product from the combustion of coal in thermal power plants, whereas
78 metakaolin is an industrial mineral product formed by the calcination of kaolinite clay.
79 However, the use of metakaolin as the aluminosilicate source in geopolymer synthesis
80 provides a relatively simpler model system for the study of geopolymers when compared to
81 the multiphase and highly variable nature of industrial aluminosilicate wastes such as fly ash,
82 In particular, metakaolin-based systems provide a more straightforward system to aid in
83 understanding the mechanisms of reaction leading to binder formation, as well as resistance
84 to chemical attack and consequently durability in service. This study builds new
85 understanding of these properties by analysing the effects of exposure to the solvents used in
86 post combustion carbon capture, on both fly ash and metakaolin based geopolymer systems.
87 It is unlikely that metakaolin-based geopolymer concretes would be seriously considered for
88 large-scale use in this type of application due to their generally high porosity, but they are
89 valuable as a means of understanding the influence of the solvents on the aluminosilicate gel
90 structure.

91

92 The chemical durability problems of traditional ordinary Portland cement based systems are
93 generally caused by the degradative changes that occur in the calcium containing phases
94 (Taylor 1997). Previous work in the analysis of the potential use of different types of concrete
95 in CCS applications considered the exposure of OPC and OPC-based composite systems to
96 the same carbon capture solvents that are analysed here (Gordon et al. 2011). Decalcification
97 occurred upon exposure to MEA, and significant carbonation occurred upon exposure to
98 K_2CO_3. However, the mechanisms controlling chemical resistance in an aluminosilicate
99 geopolymeric gel will be expected to be different, based on the very different degree of cross-
100 linking in the silicate binder gels (Duxson et al. 2007a; Abora et al. 2014).

This paper will describe the chemical characterisation of geopolymer paste samples during exposure to lean carbon capture solvents, through elemental analysis of the leaching solutions and X-ray diffractometry (XRD) of the pristine and leached materials. Lean solvents have been selected for analysis, rather than CO_2-loaded solvents, because it is more likely that concrete construction would be considered initially for use in the less chemically-aggressive parts of a carbon capture process, rather than in the more challenging environment of exposure to a rich solvent. Compressive strength data are presented to provide some insight into the influence of the leaching process on mechanical performance.

2. Materials and Methods

2.1. Sample formulations

The metakaolin used was sold under the brand name Metastar 402 by Imerys Minerals, UK. It has a BET surface area of 12.7 m^2/g and a mean particle size d_{50} of 1.58 μm (Duxson et al. 2006). The fly ash was from the Gladstone power station, Queensland, Australia and the ground granulated blast furnace slag (GGBFS) was obtained from Independent Cement & Lime, Australia. Table 1 presents the component oxide ratios for these materials.

A series of 32 geopolymer formulations were examined (Table 2). Of these, 15 were based on a mixture of metakaolin and ground granulated blast furnace slag (MK:GGBFS mass ratio 3:1) and 15 based on fly ash mixed with ground granulated blast furnace slag (FA:GGBFS mass ratio 2:1), along with a pure metakaolin-based binder and a pure fly ash-based binder. All mixes were activated with liquid sodium silicate activators, made by combining a commercial sodium silicate solution (Grade N®, PQ Australia, composition (mass basis):

124 SiO_2 28.7%, Na_2O 8.9%, H_2O 62.4%) with NaOH and Milli-Q water, to give the oxide ratios
125 shown in Table 2. Table 3 summarises the parameters which were varied in each sample set
126 in Table 2.

127

128 **2.2 Analytical methodology**

129 Leaching analysis was carried out using cylindrical sections of paste samples, which were
130 cured under sealed conditions for 48 hours at 40°C and a further 5 days at room temperature
131 (23±2°C) prior to exposure to aggressive conditions. A solid section of ~15 g weight was
132 submerged in 200 mL of solvent: either 98% monoethanolamine (MEA), 2.5 M K_2CO_3, or
133 Milli-Q grade purified water. An aliquot of 1 mL of solution was removed after 1, 3, 7, 14, 28
134 and 90 days. The volume of leachate removed was replenished with fresh solvent and a pH
135 measurement taken at each sampling. The leachate samples were diluted 10× with 10 wt.%
136 HCl solution for analysis by inductively coupled plasma-optical emission spectroscopy (ICP-
137 OES) to determine the concentrations of Al, Si, Na and Ca present.

138

139 For compressive strength testing, mortar specimens of each formulation were made with the
140 addition of sand at a 3:1 volume ratio of sand to aluminosilicate solids. These were sealed in
141 50 mm cubic moulds at 40 ^{o}C for 48 hours, then held at room temperature and maintained
142 sealed, to match the curing regime used for the paste samples. After 7 and 28 days, they were
143 analysed for compressive strength. Three replicate specimens were tested for each sample,
144 and the mean results are reported.

145

Mortar cube samples were also submerged in the solvents (98% MEA, 2.5M K_2CO_3 and Milli-Q water) for 28 days, without replenishment of the solvent, before being analysed for compressive strength; again there were three replicates for each sample and the mean result is reported.

X-ray diffraction analysis was carried out on crushed paste samples after 90 days of exposure, on a Bruker D8 Advance using Cu Kα radiation, λ = 1.5405 Å. Traces were measured at a scan speed of 5s/step and a step size of 0.02°, from 5 to 55° 2θ.

3. Results and discussion

3.1. Leaching and mechanical strength

Figures 1 and 2 show the measured extent of leaching of both Si (Figure 1) and Al (Figure 2) from all of the metakaolin-based and fly ash-based geopolymer formulations in each of the three solvents. These plots do not show sample-specific data, but instead give an overall view of the leaching resistance of each binder as a function of the solvent used. There was high resistance to MEA, with generally <1% Si and Al leaching in this solvent during the test duration. However, there was notably increased leaching of matrix components induced by alkali attack on the matrix in both K_2CO_3 and H_2O. The pH value exceeded 12 after one day of exposure in all solvents, due to release of alkalis from the pore solution of the samples, and remained at this level throughout the duration of the study. The leaching of matrix components was rapid, with the majority of the leaching taking place within the first day of exposure to all solvents. There was then a further, very gradual release of Si and Al with increased solvent ingress into the binders over time, and this effect was more marked in the fly ash formulations than the metakaolin binders, probably due to the lower w/b ratios

achievable in a mix design using spherical fly ash particles rather than plate-shaped metakaolin particles as the aluminosilicate source (Provis et al. 2010).

The main reason for the high degree of leaching observed here was that the pastes were quite immature at the point in time when they were first immersed in the solvents (i.e., 7 days of curing under sealed conditions at near-ambient temperature). This was designed to enable a comparative analysis between the dissolution of binder components within a realistic laboratory test time frame, as more mature geopolymer binders have been shown to display a much lower degree of leaching of binder components during extended exposure to alkaline solutions (Sindhunata et al. 2008; Temuujin et al. 2011). This is necessary in order to develop a scientific understanding of the influence of synthesis parameters on binder performance under these conditions, as more mature binders would be expected to show relatively less variation in nanostructure and microstructure after leaching due to the reduced influence of the solvent environment, and would thus be less instructive than the less-mature specimens investigated here.

An intermediate level of Ca content was provided to the binders studied here by the addition of granulated blast furnace slag (GGBFS). This is known to enhance the impermeability properties of the binder by the formation of a void filling, low-Ca, Al-substituted calcium silicate hydrate (C-(A)-S-H) gel in coexistence with the alkali aluminosilicate gel resulting from geopolymerisation (Kumar et al. 2010; Provis et al. 2012). The relatively low content and accessibility of calcium in the geopolymer binders is predicted to prevent the degradative effects of solvent-induced carbonation. Carbonation by gaseous CO_2-rich environments has been shown to be reasonably rapid in some alkali-activated binder systems (Puertas et al.

194 2006; Bernal et al. 2010), but the mechanism of carbonation in the fully saturated
195 environments studied here, and its influence on the binder structure, are expected to differ
196 significantly.

197

198 Previous studies of acid and alkali resistance in geopolymers found that mass and strength
199 loss occurred through leaching, correlating with the increasing porosity of the binders
200 through (Temuujin et al. 2011; Lloyd et al. 2012; McLellan et al. 2012) or alkali (Sindhunata
201 et al. 2008; Temuujin et al. 2011) attack. The leaching of Fe, Al and Na was high in acidic
202 solutions, and Si leaching dominated in alkaline conditions.

203

204 The trends displayed in Figure 1 show that the leaching of Si in K_2CO_3 in the fly ash-based
205 systems occurred more readily relative to the metakaolin-based systems, while Al leaching
206 (Figure 2) is significantly greater in water than in either of the carbon capture solvents used.
207 Perera et al. (2006) showed that the release of alkali metal cations from both fly ash and
208 metakaolin based geopolymers was high in distilled water when accompanied by hydroxide
209 leaching, and the pH, both in that study and in our experiments, was found to be greater than
210 12 throughout the test period. It is possible that the presence of carbonate at this pH is
211 suppressing the solubility of $Al(OH)_4^-$, most likely by increasing the ionic strength of the
212 solution.

213

214 Figure 3 shows the total Si, Al, Na and Ca leached, expressed as a percentage of the total
215 inventory of each element in the samples, after 90 days of exposure.

216

If each oxide ratio series is viewed separately (Table 3), Si leaching increases through the series with increasing SiO_2/Al_2O_3 ratio (2Na-4Na for MK/GGBFS and 18-22Na for FA/GGBFS) in all solvents. This is also accompanied by a loss in compressive strength (Figure 4). The strength loss is attributed to the reduced availability of Al for reaction, which is known to control the strength properties of geopolymers (Weng et al. 2005; Fernández-Jiménez et al. 2006; Duxson et al. 2007a). Aly *et al*. (2008) proposed that a lower degree of polymerisation occurs at higher Si/Al ratios, and supported this proposal using ^{29}Si and ^{27}Al magic angle spinning nuclear magnetic resonance (MAS NMR) spectroscopy: a reduced influence of Al on the average Si coordination sphere was observed, and XRD and infrared spectroscopic data also indicated a structural shift towards amorphous silica with increasing Si/Al ratio. This indicates that the correlation between reduced strength and increased leaching of Si is due to the reduced extent of geopolymerisation reactions within these immature binders, as the extent of incorporation of Si into the binder itself is not yet high.

However, the correlation between more marked strength loss and increased leaching does not follow for all of the binders. For example, the leaching extents observed in samples 7Na and 23Na are the lowest in their respective series (Figure 3), but unexposed strength was low in 7Na (~13 MPa) after 28 days of aging, and exposure to MEA resulted in catastrophic strength loss (Figure 4). The same trend is observed in sample 23Na (strengths of <5 MPa, no residual strength in water or K_2CO_3). This may be related to the low extent of reaction of the aluminosilicate precursors, as both of these specimens are formulated specifically to test the effect of a reduction in the Na_2O/SiO_2 ratio; i.e., a reduction in activator alkalinity, and thus reduced extent of interaction with the aluminosilicate particles during the geopolymerisation reaction. It is therefore necessary to consider this process to bring understanding of the formation, and subsequent degradation by leaching, of geopolymer binders.

242

243 Previous studies have considered the rate and extent of dissolution of fly ash in alkaline
244 media, which is central to this discussion. Li *et al*. (2011) showed that the extent of fly ash
245 dissolution in NaOH solutions was relatively low, even at high NaOH concentrations (6.0-
246 13.4 M). In that study, the dissolution of Al occurred more readily than Si, shown by the
247 variation of Si/Al ratio over time (Li et al. 2011) but in an earlier study (Pietersen et al.
248 1989), congruent dissolution was observed. It appears that the details of this process depend
249 on the specific chemistry of the fly ash under analysis, and also the leaching environment
250 used; Phair and van Deventer (2001) tested the leaching of Si and Al from a fly ash sourced
251 from the same power station as the material used here, and found that the degree of
252 incongruency of dissolution (favouring more rapid Al release) generally decreased with
253 increasing NaOH concentration. Here, at the lowest alkali concentrations tested (sample 7Na
254 in the fly ash system), it appears that the binder after 7 days of curing is sufficiently immature
255 that the concentration of gel (which is the part of the material susceptible to solvent leaching)
256 is low enough to give an apparently low extent of overall leaching, in parallel with poor
257 strength performance. For the case of the metakaolin samples (particularly 13Na), the
258 situation is broadly similar. Additionally, previous leaching studies have observed
259 reprecipitation of aluminosilicate gels during leaching of geopolymers in alkaline solutions
260 (Sindhunata et al. 2008), and this may also partially explain the low leaching rate found here
261 when high strength loss and structural damage have occurred.

262

263 Where the Na_2O/SiO_2 ratio is increased (samples 7Na-9Na for MK/GGBFS and 23Na-27Na
264 for FA/GGBFS), variation in water content was required to hold H_2O/Na_2O constant with the
265 increase in alkalinity. As noted above, Sindhunata *et al.* (2008) observed reprecipitation of

aluminosilicate species when geopolymers were exposed to highly alkaline solutions, but this effect was reduced marked at very high alkalinity. There is increased leaching of Si when increasing the Na_2O/SiO_2 ratio in the fly ash sample series (23Na-27Na, Figure 3e), which is assigned in part to the increased formation of geopolymer gel at higher alkalinity, and in part to the higher water content, which would be expected to increase porosity and permeability and thus increase alkali attack.

Correspondingly, the samples where the water content was the sole parameter varied (13Na-16Na and 28Na-32Na) do show a trend towards reduction in strength at increased water content (Figure 4). The generally increased leaching of Si follows in the fly ash formulations (28Na-32Na), Figure 3e. However, leaching remains low and follows no particularly apparent trend with respect to water content in the metakaolin binders; reprecipitation of aluminosilicate gels is likely to provide an explanation for this observation. The leaching of Al is significantly higher in water than in K_2CO_3. The samples with very low leaching of Al (28Na-31Na, Figure 3f) are those that have both high unexposed and residual strengths.

The amount of Na leached is higher than all the other ions for every formulation, which is related to the high mobility rate of those ions compared to the other ones studied, as Na is present largely in the pore solution of the materials, and in weakly associated charge-balancing sites (Lloyd et al. 2010). Further, the leaching of Na is significantly lower in MEA compared to H_2O and K_2CO_3, as MEA is a less effective solvent than aqueous environments for alkali hydroxides. For the fly ash formulations, no clear trends can be observed in the MEA solution. However in water and K_2CO_3 there is decreased leaching of Na with increased Na_2O/SiO_2 ratio in the fly ash sample series (23Na-27Na) which is contrary to the

behaviour of Si and Al (Figure 3g) where increased leaching is attributed to the higher water content and assumed higher porosity through this series. The higher alkalinity of these systems results in greater production of geopolymer gel and so possibly the Na is chemically bound within the pore structure through the electrostatic interactions with the geopolymer matrix. Na is increasingly leached when the H_2O/SiO_2 ratio increases (28Na-32Na), due to the higher water content.

The significant observed extent of Ca leaching (Figure 3d,h) shows that a significant proportion of the Ca present is available for leaching by the solvent solutions. Previous work has shown that significant decalcification occurs in OPC, OPC/GGBFS and OPC/FA binders on exposure to MEA (Gordon et al. 2011), so these data show that the Ca-containing gels formed in these geopolymer systems seem to release Ca in a similar manner. X-ray diffraction data, presented below, show that in addition to the Ca present as dissolved species in the leaching solution, additional Ca is removed from the gel binder and precipitated in the formation of calcite ($CaCO_3$) on exposure to K_2CO_3, and also due to atmospheric carbonation in a few samples where the seal on the leaching vessel had been breached during sampling throughout the testing period.

3.2. X-ray diffraction

Figures 5-6, and the Supporting Information, show XRD traces for the metakaolin/GGBFS based binders, with separate figures focusing on each series of oxide ratios and their exposure under different conditions (Table 2), and compared to the binders of the same formulation which were aged at room temperature under sealed conditions for durations corresponding to the solvent exposure tests.

315

316 Figure 5 presents data for samples 2Na-4Na. The muscovite ($KAl_2(Si,Al)_4O_{10}(OH)_2$,
317 PDF#58-2035) was present as an impurity in the metakaolin used, and reacts only slightly
318 during geopolymer formation (Yip et al. 2008). The mixed carbonate - bicarbonate phase
319 trona $Na_3(CO_3)(HCO_3)\cdot 2H_2O$ formed on the surface of the pure metakaolin sample 1Na and
320 also on the surfaces of samples 1Na-4Na through atmospheric exposure, possibly in the initial
321 curing stage when the samples were held at 40 °C for 48 hours as this phase is
322 thermodynamically more stable at temperatures slightly higher than room temperature
323 (Bernal et al. 2012). Pirssonite $CaNa_2(CO_3)\cdot 2(H_2O)$, formed by atmospheric carbonation, was
324 also detected in samples 3Na (and thus is shown in the corresponding plots as 9Na and 14Na)
325 and also in sample 12Na, but was not detected in these samples following solvent exposure.
326 However, it has formed in sample 15Na following exposure to MEA, although this may also
327 have been due to some atmospheric carbonation prior to or during XRD analysis.

328

329 A zeolite phase, faujasite (approximately $Na_2Al_2Si_{3.3}O_{10}\cdot 7H_2O$, PDF# 12-0228) has formed in
330 all samples. At the highest SiO_2/Al_2O_3 ratio a Na-chabazite zeolite phase (approximately
331 $NaAlSi_2O_6\cdot 3H_2O$, PDF# 19-1178) has also formed. Very little zeolite was detected in all
332 samples following solvent exposure, with only small faujasite peaks detected in sample 3Na
333 following exposure to H_2O. This appears to be related to the limited extent of zeolite
334 formation observed after 7 days of curing (where the residual activator in the pores was
335 washed out during immersion in water, effectively stopping the geopolymerisation/zeolite
336 growth reaction), rather than via the removal of zeolitic phases during immersion. A study of
337 accelerated aging of geopolymers (Lloyd 2009) showed that at 23°C there was no zeolite
338 crystallisation in a metakaolin geopolymer for up to 3 months of aging. That study also

considered the relationship between zeolite formation and strength retention in geopolymeric systems, concluding that the strongest correlation is between pore network stability and strength retention, rather than observing a direct link between zeolite evolution and geopolymer strength. Palomo et al. (1999) also exposed immature alkali activated metakaolin geopolymer to aggressive solutions, where the binders had been subjected to accelerated curing (85 °C) for just 2 days prior to exposure, and also found faujasite across a wide range of pH conditions, but not until at least 3 months of exposure in the samples immersed at high pH.

Zeolite formation within geopolymer binders is a complex process (Provis et al. 2005) and not yet fully understood. However, the formation of Na-chabazite along with faujasite in only sample 4Na (Figure 5a) is attributed to the increased Si/Al ratio of this sample. The high Si/Al ratio, reduced extent of geopolymerisation and alkali-rich pore solution conditions lead to the coexistence of these zeolitic phases (faujasite and chabazite), which is not observed in the formulations with less Si.

Solvent exposure in general inhibits the formation of zeolites compared to the unexposed samples, most likely due to the removal or dilution of the alkaline pore fluids required for ongoing reaction within the geopolymer gel. Exposure to MEA (Figure 5b) left muscovite as the only crystalline phase observed in the samples, while the amorphous 'hump' characteristic of the disordered aluminosilicate geopolymer framework (Provis et al. 2005) remains intact. This is in good agreement with the low level of leaching of both Si and Al found on exposure to MEA in all samples.

363 Exposure to water (Figure 5c) has also hindered the development of zeolitic phases through
364 the dilution of the pore solution, and some carbonation, evident via the formation of
365 crystalline calcite ($CaCO_3$, PDF #05-0586) occurred in samples 2Na and 3Na after exposure
366 to water and K_2CO_3, showing that calcium is available for reaction with the atmosphere. This
367 is in good agreement with the high leachability of Ca as observed in all solvents (Figure 3d).
368 No zeolitic phases form during exposure to K_2CO_3 (Figure 5d), apart from a small amount of
369 faujasite detected in samples 2Na and 3Na, which also forms in these formulations following
370 exposure to water (Figure 5c).
371
372 Figure 6, which shows XRD data for the sample series with increasing Na_2O/SiO_2 ratio,
373 demonstrates the formation of faujasite in samples 8Na and 9Na. No zeolitic phases have
374 formed in sample 7Na (Figure 6a), which has the lowest Na_2O content; the lower extent of
375 reaction of the aluminosilicate precursor phases in this system will affect the availability of
376 species for zeolite crystallisation. Additionally, in this sample there was also a reduction in
377 water content in order to achieve the Na_2O/SiO_2 ratio required, and this too may be
378 significant in inhibiting the formation of zeolites, as steric restrictions may reduce the growth
379 of germ nuclei which lead to the formation of crystalline zeolites (Barrer 1981; Provis et al.
380 2005). Sample 7Na also shows a small degree of atmospheric carbonation, seen through the
381 formation of aragonite, a metastable polymorph of $CaCO_3$.
382
383 Following exposure to solvents, a significant quantity of faujasite develops only in 8Na after
384 exposure to MEA (Figure 6b) and water (Figure 6c). A smaller quantity of faujasite is seen in
385 the 9Na formulation exposed to water, and slight traces in 9Na following exposure to K_2CO_3
386 (Figure 6d). Significant calcite formation is again observed during K_2CO_3 exposure (Figure

387 6d) through decalcification, and kalcinite ($KHCO_3$, PDF # 12-0297) has also formed in all
388 K_2CO_3 exposed samples through the reaction of K_2CO_3 with CO_2 and H_2O. Corresponding
389 data and additional discussion related to the metakaolin sample series with increasing
390 H_2O/SiO_2 ratios are presented as Supporting Information (Figure S1 and associated text).
391 These data show the formation of zeolites in each sample, although their prevalence is
392 reduced by K_2CO_3 exposure, which appears to hinder the structural evolution and
393 crystallisation of the zeolites.

394

395 The XRD data for the fly ash-based formulations are presented in Figures 7-8 and in the
396 Supporting Information, again divided by oxide ratio series as outlined in Table 2. In these
397 samples, a basic Na-sodalite phase (approximately, $1.08Na_2O{\cdot}Al_2O_3{\cdot}1.68SiO_2{\cdot}1.8H_2O$, PDF#
398 31-1271) was formed; this is a feldspathoid structure, closely related to zeolites, and appears
399 to be present in all samples regardless of solvent exposure. Sample 17Na, the pure fly ash
400 binder, also contains trona ($Na_3(CO_3)(HCO_3){\cdot}2H_2O$) as a product of slight atmospheric
401 carbonation. Also present in all of the fly ash based formulations were the unreactive phases
402 supplied by the fly ash, being quartz and mullite.

403

404 Figure 7 shows the data for the sample series with increasing SiO_2/Al_2O_3 ratio. The formation
405 of basic sodalite appears to reduce as the Si content increases, likely due to the reduction in
406 Al available for crystallisation, as this phase forms with $SiO_2/Al_2O_3 = 2$ and so requires high
407 Al availability for crystallisation. The sodalite appears to be largely unaffected by exposure to
408 MEA (Figure 7b). Si and Al leaching was also low for the fly ash formulations immersed in
409 MEA (Figures 1 and 2), and residual strength on exposure to solvents was high (Figure 4). It
410 therefore seems that for the fly ash formulations, 28 days of exposure to MEA has not

411 significantly altered the expected path of microstructural development, with the slight losses
412 in strength attributed to alkali attack on the framework.

413

414 The basic sodalite phase also develops in almost all samples following exposure to water
415 (Figure 7c), but in concentrations again decreasing though the sample series. However,
416 sample 18Na showed instead the formation of a faujasite phase as the main zeolitic product,
417 similar to the fly ash-only sample 17Na. Sample 18Na had the lowest Si/Al ratio of the
418 samples in this series. However, faujasite was not formed in the 18Na sample subjected to
419 other immersion conditions, so its formation here may be due to the effectively increased
420 water content on immersion, and the effect of the subsequent diffusion of the contents of the
421 pore solution out into the leaching solution. Exposure to water is also accompanied by a
422 significant amount of carbonation, with the formation of calcite in all samples of the fly ash-
423 slag series.

424

425 A small amount of sodalite was also formed on exposure to K_2CO_3 (Figure 7d). Carbonation
426 also occurred in all samples exposed to K_2CO_3 with the formation of calcite $CaCO_3$ (PDF#
427 47-1743) through decalcification and kalcinite, $KHCO_3$ (PDF# 12-0292) through reaction of
428 K_2CO_3, CO_2 and H_2O. Some crystalline K_2CO_3 (PDF# 70-0292) also precipitated in all
429 samples. The high leachability of Na and Si in K_2CO_3 (Figure 3) resulted in total strength loss
430 after 28 days of solvent exposure (Figure 4), and this is consistent with the notable reduction
431 in the amorphous 'hump' corresponding to the geopolymer gel in this leaching environment
432 in particular (Figure 7d). The microstructural development has been significantly affected
433 following 28 days of exposure to K_2CO_3, but despite this the mechanism of zeolite formation

found in the unexposed samples still persists, although to a lesser extent due to the leaching processes taking place.

The XRD data for the series with increasing Na_2O/SiO_2 ratio are given in Figure 8. In the unexposed samples (Figure 8a), basic sodalite is more prominent with increasing Na content, with the exception of sample 27Na. In this formulation, the hydroxide and water contents are highest, and there is no trace of sodalite, but faujasite has formed instead. In sample 23Na, where hydroxide and water contents are low, no zeolitic phase has formed. Again, there is very little effect on the microstructure induced by exposure to MEA (Figure 8b) or water (Figure 8c). The same zeolites as in the unexposed samples, faujasite (in 27Na) and basic sodalite (in 24Na-26Na), have again developed (but to a lesser extent than in the unexposed samples) after exposure to K_2CO_3 (Figure 8d).

The XRD data for the series with increasing H_2O/SiO_2 ratio are shown in the Supporting Information. Basic sodalite was formed in all of the unexposed samples, and there appears to be very little difference in the crystalline phases formed, other than calcite formation in all samples, and slight suppression of crystallisation by K_2CO_3 immersion. This series had the highest unexposed and also residual strengths upon exposure after 28 days of immersion, and it appears that these five samples have the least alteration in crystallographic structure among those studied.

3.3 Implications

The specimens tested here show notable degradation under exposure to carbon capture solvents, and as such would not be directly useful in applications where they are brought into immediate contact with these solvents in service. However, this was a part of the design of this study, which is in effect an accelerated test to simulate a worst-case leaching scenario. The resistance of geopolymers to alkali attack and carbonation would certainly be higher if more mature binders were tested, but the aim of this study has been to elucidate the degradation mechanisms through induction of artificially rapid degradation processes. The key to geopolymer concrete durability in carbon capture applications will be the development of low porosity and high tortuosity of the pore structure, in order to reduce the accessibility of the key binder phases. A forthcoming study will directly address the pore network geometry of these binder systems, and provide further insight into this important issue. In any case, the results of this study show that the resistance of geopolymers to attack by aqueous K_2CO_3 is not as high as was predicted based upon nanostructural arguments, and this solvent does cause significant damage to the aluminosilicate geopolymer framework.

4. Conclusions

Alkali activated geopolymer concretes may provide a cost saving alternative construction material for use in place of large stainless steel vessels in carbon capture facilities. This study was based around the study of immature and relatively porous binders, in order to best understand the mechanism of chemical attack on geopolymers during exposure to carbon capture solvents. Leaching occurred rapidly, within one day of immersion, due to the release of alkalis from the pore solution and attack on loosely bound Si and Al species within these immature binders. Resistance to MEA is highest among the solvents tested, with low solubility of Na in this solvent.

The microstructural development of the metakaolin/slag geopolymer formulations was more significantly affected by solvent immersion than was the structure of the fly ash/slag geopolymers. Solvent immersion seems to suppress the formation of faujasite in the metakaolin/slag binders, and the residual strength of these binders is relatively low. However, the formation of basic sodalite, which is the predominant crystalline phase observed in the fly ash/slag formulations, is much less influenced by solvent immersion, particularly in the case of immersion in MEA or water, where the 28 day residual strength is high. The reduced extent of binder development observed on exposure to K_2CO_3 (evidenced by the lower degree of zeolite formation and also the dissolution of much of the amorphous geopolymer gel phase), along with the effects of significant carbonation does, in the majority of cases, caused catastrophic strength failure of the matrix on exposure to K_2CO_3.

5. Acknowledgements

The authors acknowledge the funding provided by the Australian Government through its CRC Program for this CO2CRC research project, and the salary support of JLP provided through the Discovery Grants program via APD and DORA Fellowships.

6. References

Abora, K., Beleña, I., Bernal, S.A., Dunster, A., Nixon, P.A., Provis, J.L., Tagnit-Hamou, A. and Winnefeld, F. (2014). Durability and testing - Chemical matrix degradation processes. in: Alkali-Activated Materials: State-of-the-Art Report, RILEM TC 224-AAM. Eds. J.L. Provis and J.S.J. van Deventer. Dordrecht, Springer/RILEM**:** 177-221.

507 Aly, Z., Vance, E.R., Perera, D.S., Hanna, J.V., Griffith, C.S., Davis, J. and Durce, D. (2008).
508 "Aqueous leachability of metakaolin-based geopolymers with molar ratios of
509 Si/Al=1.5-4." Journal of Nuclear Materials **378**(2): 172-179.

510 Bakharev, T. (2005). "Resistance of geopolymer materials to acid attack." Cement and
511 Concrete Research **35**(4): 658-670.

512 Barrer, R.M. (1981). "Zeolites and their synthesis." Zeolites **1**(3): 130-140.

513 Bernal, S.A., Mejía de Gutiérrez, R., Provis, J.L. and Rose, V. (2010). "Effect of silicate
514 modulus and metakaolin incorporation on the carbonation of alkali silicate-activated
515 slags." Cement and Concrete Research **40**(6): 898-907.

516 Bernal, S.A., Provis, J.L., Brice, D.G., Kilcullen, A., Duxson, P. and van Deventer, J.S.J.
517 (2012). "Accelerated carbonation testing of alkali-activated binders significantly
518 underestimates service life: The role of pore solution chemistry." Cement and
519 Concrete Research **42**(10): 1317-1326.

520 Davidovits, J. (1991). "Geopolymers - Inorganic polymeric new materials." Journal of
521 Thermal Analysis **37**(8): 1633-1656.

522 Duxson, P., Fernandez-Jimenez, A., Provis, J.L., Lukey, G.C., Palomo, A. and van Deventer,
523 J.S.J. (2007a). "Geopolymer technology: the current state of the art." Journal of
524 Materials Science **42**(9): 2917-2933.

525 Duxson, P., Lukey, G.C. and van Deventer, J.S.J. (2006). "Thermal evolution of metakaolin
526 geopolymers: Part 1 - Physical evolution." Journal of Non-Crystalline Solids **352**(52-
527 54): 5541-5555.

528 Duxson, P., Provis, J.L., Lukey, G.C. and Van Deventer, J.S.J. (2007b). "The role of
529 inorganic polymer technology in the development of 'green concrete'." Cement and
530 Concrete Research **37**(12): 1590-1597.

531 Fernández-Jiménez, A. and Palomo, A. (2009). Chemical durability of geopolymers. in:
532 Geopolymers: Structure, Processing, Properties and Industrial Applications. Eds. J.L.
533 Provis and J.S.J. van Deventer. Cambridge, UK, Woodhead**:** 167-193.

534 Fernández-Jiménez, A., Palomo, A., Sobrados, I. and Sanz, J. (2006). "The role played by the
535 reactive alumina content in the alkaline activation of fly ashes." Microporous and
536 Mesoporous Materials **91**(1-3): 111-119.

537 Gordon, L.E., Provis, J.L. and van Deventer, J.S.J. (2011). "Durability of fly ash/GGBFS
538 based geopolymers exposed to carbon capture solvents." Advances in Applied
539 Ceramics **110**(8): 446-452.

540 Jenkins, C.R., Cook, P.J., Ennis-King, J., Undershultz, J., Boreham, C., Dance, T., de Caritat,
541 P., Etheridge, D.M., Freifeld, B.M., Hortle, A., Kirste, D., Paterson, L., Pevzner, R.,
542 Schacht, U., Sharma, S., Stalker, L. and Urosevic, M. (2012). "Safe storage and
543 effective monitoring of CO_2 in depleted gas fields." Proceedings of the National
544 Academy of Sciences of the United States of America **109**(2): E35-E41.

545 Juenger, M.C.G., Winnefeld, F., Provis, J.L. and Ideker, J.H. (2011). "Advances in alternative
546 cementitious binders." Cement and Concrete Research **41**(12): 1232-1243.

547 Kumar, S., Kumar, R. and Mehrotra, S.P. (2010). "Influence of granulated blast furnace slag
548 on the reaction, structure and properties of fly ash based geopolymer." Journal of
549 Materials Science **45**(3): 607-615.

550 Li, C., Li, Y., Sun, H. and Li, L. (2011). "The composition of fly ash glass phase and its
551 dissolution properties applying to geopolymeric materials." Journal of the American
552 Ceramic Society **94**(6): 1773-1778.

553 Lloyd, R.R. (2009). Accelerated ageing of geopolymers. in: Geopolymers: Structure,
554 Processing, Properties and Industrial Applications. Eds. J.L. Provis and J.S.J. van
555 Deventer. Cambridge, UK, Woodhead**:** 139-166.

556 Lloyd, R.R., Provis, J.L. and van Deventer, J.S.J. (2010). "Pore solution composition and
557 alkali diffusion in inorganic polymer cement." Cement and Concrete Research **40**(9):
558 1386-1392.

559 Lloyd, R.R., Provis, J.L. and van Deventer, J.S.J. (2012). "Acid resistance of inorganic
560 polymer binders. 1. Corrosion rate." Materials and Structures **45**(1-2): 1-14.

561 McLellan, B.C., Corder, G.D., Giurco, D.P. and Ishihara, K.N. (2012). "Renewable energy in
562 the minerals industry: a review of global potential." Journal of Cleaner Production **32**:
563 32-44.

564 Olivier, J.G.J., Janssens-Maenhout, G. and Peters, J.A.H.W. (2012). Trends in global CO_2
565 emissions; 2012 Report. The Hague, Netherlands, PBL Netherlands Environmental
566 Assessment Agency**:** 40 pp.

567 Palomo, A., Blanco-Varela, M.T., Granizo, M.L., Puertas, F., Vazquez, T. and Grutzeck,
568 M.W. (1999). "Chemical stability of cementitious materials based on metakaolin."
569 Cement and Concrete Research **29**(7): 997-1004.

570 Perera, D.S., Vance, E.R., Aly, Z., Davis, J. and Nicholson, C.L. (2006). Immobilization of
571 Cs and Sr in geopolymers with Si/Al molar ratio of ~2. in: Environmental Issues and
572 Waste Management Technologies in the Ceramic and Nuclear Industries XI (Ceramic
573 Transactions Vol. 176), John Wiley & Sons**:** 91-96.

574 Phair, J.W. and van Deventer, J.S.J. (2001). "Effect of silicate activator pH on the leaching
575 and material characteristics of waste-based inorganic polymers." Minerals
576 Engineering **14**(3): 289-304.

577 Pietersen, H.S., Fraay, A.L.A. and Bijen, J.M. (1989). Reactivity of fly ash at high pH. 1989
578 Materials Research Society Fall Meeting (MRS Proceedings Vol. 178), Boston, MA,
579 Cambridge University Press.

580 Provis, J.L. (2014). "Geopolymers and other alkali activated materials - Why, how, and
581 what?" Materials and Structures **47**(1): 11-25.

582 Provis, J.L., Duxson, P. and van Deventer, J.S.J. (2010). "The role of particle technology in
583 developing sustainable construction materials." Advanced Powder Technology **21**(1):
584 2-7.

585 Provis, J.L., Lukey, G.C. and van Deventer, J.S.J. (2005). "Do geopolymers actually contain
586 nanocrystalline zeolites? A reexamination of existing results." Chemistry of Materials
587 **17**(12): 3075-3085.

588 Provis, J.L., Myers, R.J., White, C.E., Rose, V. and van Deventer, J.S.J. (2012). "X-ray
589 microtomography shows pore structure and tortuosity in alkali-activated binders."
590 Cement and Concrete Research **42**(6): 855-864.

591 Provis, J.L. and van Deventer, J.S.J., Eds. (2014). Alkali-Activated Materials: State-of-the-
592 Art Report, RILEM TC 224-AAM. Dordrecht, Springer/RILEM.

593 Puertas, F., Palacios, M. and Vazquez, T. (2006). "Carbonation process of alkali-activated
594 slag mortars." Journal of Materials Science **41**(10): 3071-3082.

595 Sindhunata, Provis, J.L., Lukey, G.C., Xu, H. and van Deventer, J.S.J. (2008). "Structural
596 evolution of fly ash based geopolymers in alkaline environments." Industrial &
597 Engineering Chemistry Research **47**(9): 2991-2999.

598 Taylor, H.F.W. (1997). Cement Chemistry, 2nd Ed. London, UK, Thomas Telford.

599 Temuujin, J., Minjigmaa, A., Lee, M., Chen-Tan, N. and van Riessen, A. (2011).
600 "Characterisation of class F fly ash geopolymer pastes immersed in acid and alkaline
601 solutions." Cement & Concrete Composites **33**(10): 1086-1091.

602 van Deventer, J.S.J., Provis, J.L. and Duxson, P. (2012). "Technical and commercial progress
603 in the adoption of geopolymer cement." Minerals Engineering **29**: 89-104.

604 van Deventer, J.S.J., Provis, J.L., Duxson, P. and Brice, D.G. (2010). "Chemical research and
605 climate change as drivers in the commercial adoption of alkali activated materials."
606 Waste and Biomass Valorization **1**(1): 145-155.

607 Weng, L.Q., Sagoe-Crentsil, K., Brown, T. and Song, S.H. (2005). "Effects of aluminates on
608 the formation of geopolymers." Materials Science and Engineering B-Solid State
609 Materials for Advanced Technology **117**(2): 163-168.

610 Yip, C.K., Provis, J.L., Lukey, G.C. and van Deventer, J.S.J. (2008). "Carbonate mineral
611 addition to metakaolin-based geopolymers." Cement & Concrete Composites **30**(10):
612 979-985.

613

614

615

616 Table 1. Compositions of aluminosilicate sources; wt.% as oxides, determined by X-ray
617 fluorescence. LOI is loss on ignition at 1000 °C.

	Metakaolin	**Fly ash**	**GGBFS**
SiO_2	52.8	45.5	32.9
Al_2O_3	39.2	27.8	13.2
CaO	0.1	5.6	40.1
Na_2O	0.0	0.3	0.3
K_2O	2.7	0.5	0.3
Fe_2O_3	0.8	11.2	0.3
MgO	0.2	1.4	6.0
P_2O_5	0.1	0.5	0.0
SO_3	0.0	0.2	3.5
TiO_2	0.0	1.4	0.7
MnO	0.0	0.2	0.0
LOI	1.2	2.7	1.2

618

619

620 Table 2. Component molar oxide ratios, NaOH concentrations and water/binder ratios (w/b;
621 'binder' is defined as the solid aluminosilicate precursor) of the geopolymer formulations
622 tested.

Solid aluminosilicate	ID	SiO_2/Al_2O_3	Na_2O/SiO_2	H_2O/Na_2O	NaOH (M)	w/b
MK	1Na	3.0	0.5	13.0	6.9	0.44
MK:GGBFS 3:1	2Na	3.0	0.5	13.0	7.2	0.44
MK:GGBFS 3:1	3Na	3.3	0.5	13.0	6.9	0.44
MK:GGBFS 3:1	4Na	3.6	0.5	13.0	6.6	0.45
MK:GGBFS 3:1	7Na	3.3	0.33	13.0	6.0	0.37
MK:GGBFS 3:1	8Na	3.3	0.4	13.0	6.5	0.40
MK:GGBFS 3:1	9Na	3.3	0.5	13.0	6.9	0.44
MK:GGBFS 3:1	12Na	3.3	0.5	11.0	8.2	0.40
MK:GGBFS 3:1	13Na	3.3	0.5	12.0	7.5	0.42
MK:GGBFS 3:1	14Na	3.3	0.5	13.0	6.9	0.44
MK:GGBFS 3:1	15Na	3.3	0.5	14.0	6.4	0.46
MK:GGBFS 3:1	16Na	3.3	0.5	15.0	6.0	0.48
FA	17Na	3.33	0.45	8.0	10.6	0.32
FA:GGBFS 2:1	18Na	3.1	0.45	8.0	12.2	0.32
FA:GGBFS 2:1	19Na	3.2	0.45	8.0	12.0	0.32
FA:GGBFS 2:1	20Na	3.33	0.45	8.0	11.7	0.33
FA:GGBFS 2:1	21Na	3.4	0.45	8.0	11.6	0.33
FA:GGBFS 2:1	22Na	3.5	0.45	8.0	11.4	0.33
FA:GGBFS 2:1	23Na	3.33	0.30	8.0	10.3	0.24
FA:GGBFS 2:1	24Na	3.33	0.36	8.0	10.9	0.27
FA:GGBFS 2:1	25Na	3.33	0.45	8.0	11.7	0.33
FA:GGBFS 2:1	26Na	3.33	0.6	8.0	12.1	0.36
FA:GGBFS 2:1	27Na	3.33	0.9	8.0	12.7	0.42
FA:GGBFS 2:1	28Na	3.33	0.45	7.0	13.4	0.27
FA:GGBFS 2:1	29Na	3.33	0.45	8.0	11.7	0.33
FA:GGBFS 2:1	30Na	3.33	0.45	9.0	10.4	0.33
FA:GGBFS 2:1	31Na	3.33	0.45	10.0	9.4	0.35
FA:GGBFS 2:1	32Na	3.33	0.45	11.0	8.5	0.37

623 [a] Samples shaded in grey are the same mix (one in the metakaolin-based sample set and one in the fly ash-based
624 sample set), replicated and renumbered each time in the sample listing to place this composition in the correct
625 position in the series in which each of the synthesis parameters was varied.

626

627

628

629 Table 3. Summary of sample series and the parameters varied in each.

Series	Aluminosilicate source	Parameter
2Na-4Na	Metakaolin-slag	Increasing SiO_2/Al_2O_3
7Na-9Na	Metakaolin-slag	Increasing Na_2O/SiO_2 (and w/b)
12Na-16Na	Metakaolin-slag	Increasing w/b
18Na-22Na	Fly ash-slag	Increasing SiO_2/Al_2O_3
23Na-27Na	Fly ash-slag	Increasing Na_2O/SiO_2 (and w/b)
28Na-32Na	Fly ash-slag	Increasing w/b

630

631

632

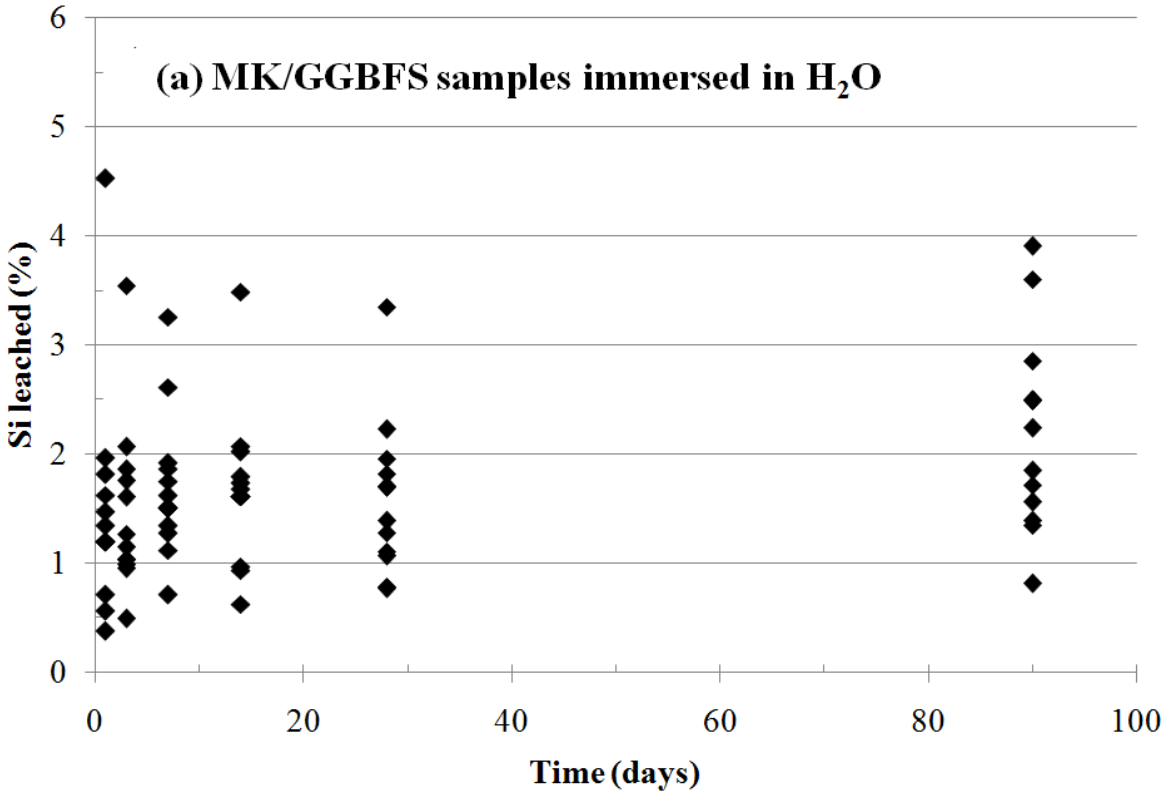
(a) MK/GGBFS samples immersed in H_2O
Si leached (%)
Time (days)
0
1
2
3
4
5
6
0
20
40
60
80
100

633

634

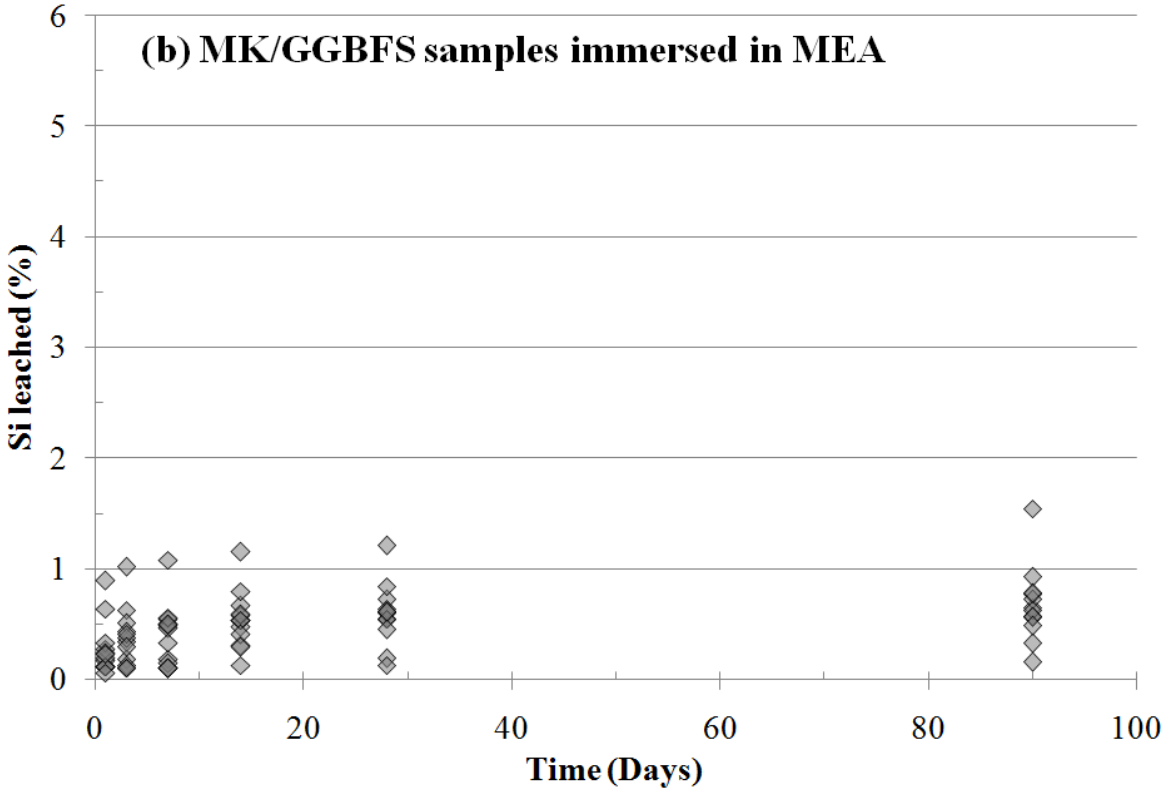
(b) MK/GGBFS samples immersed in MEA
Si leached (%)
Time (Days)
0
1
2
3
4
5
6
0
20
40
60
80
100

635

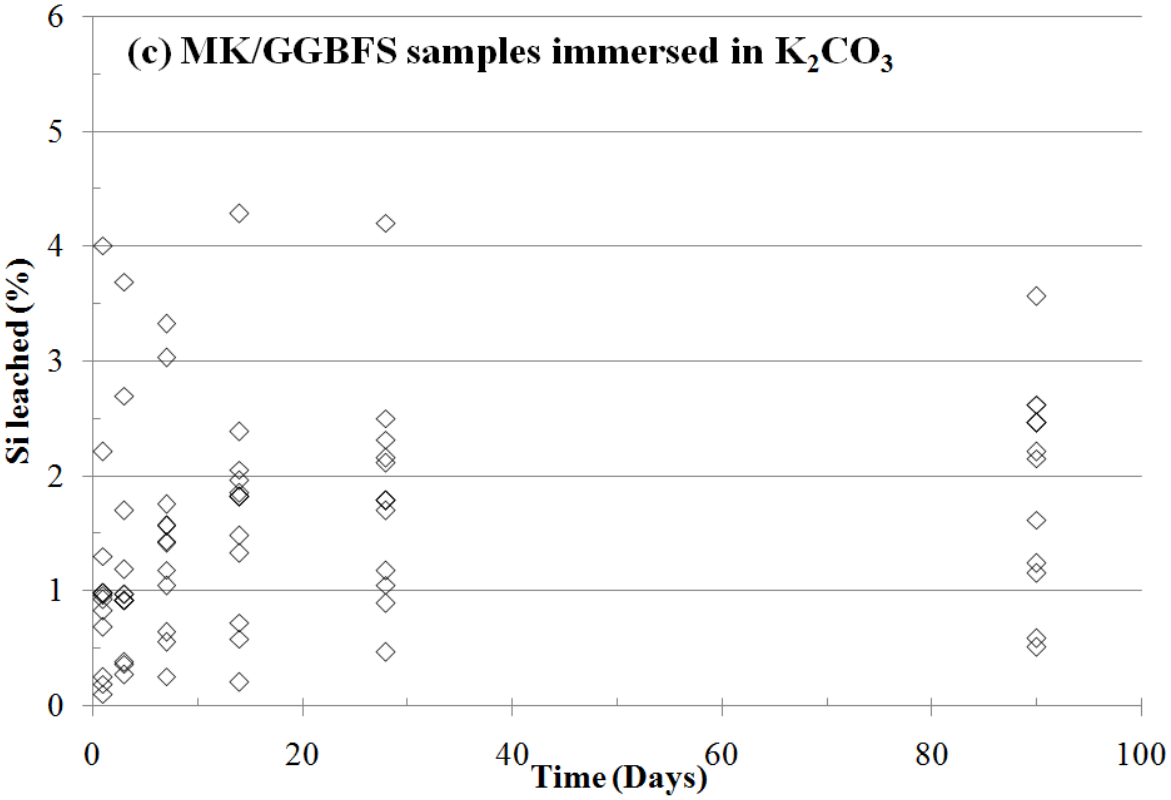
(c) MK/GGBFS samples immersed in K_2CO_3
Si leached (%)
Time (Days)
0
1
2
3
4
5
6
0
20
40
60
80
100

636

637

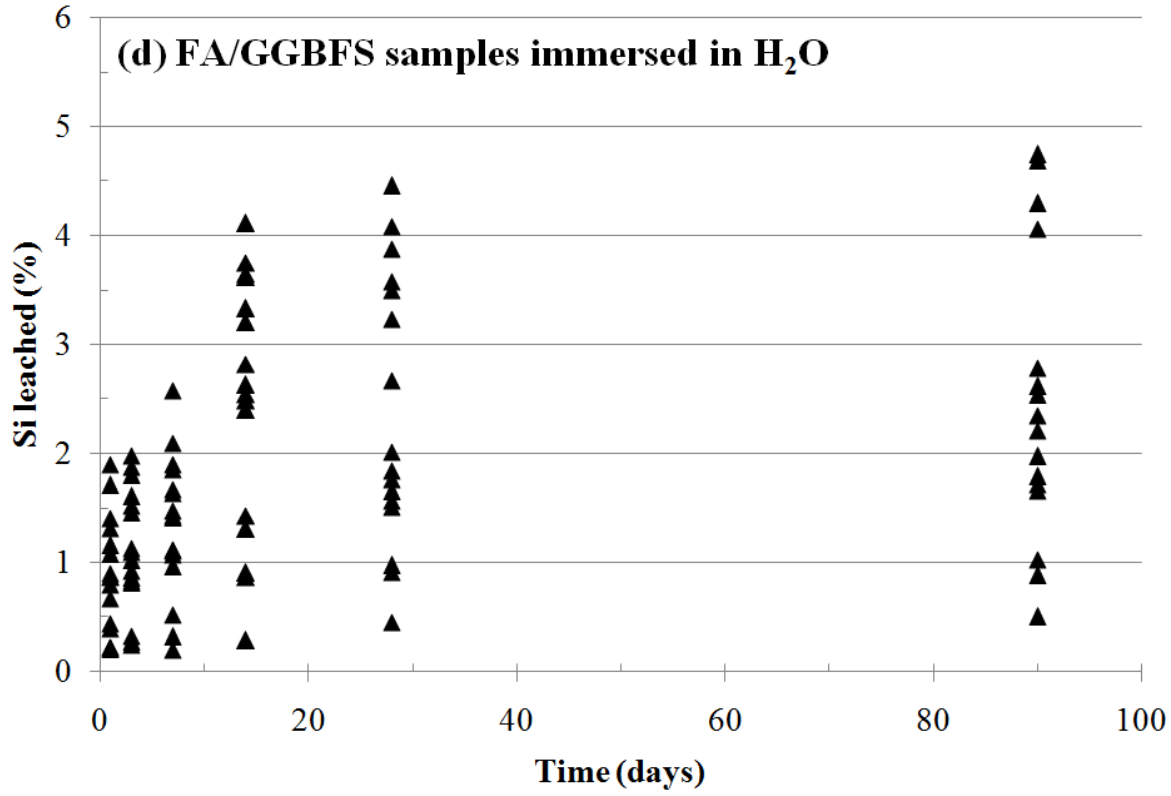
(d) FA/GGBFS samples immersed in H_2O
Si leached (%)
Time (days)
0
1
2
3
4
5
6
0
20
40
60
80
100

638

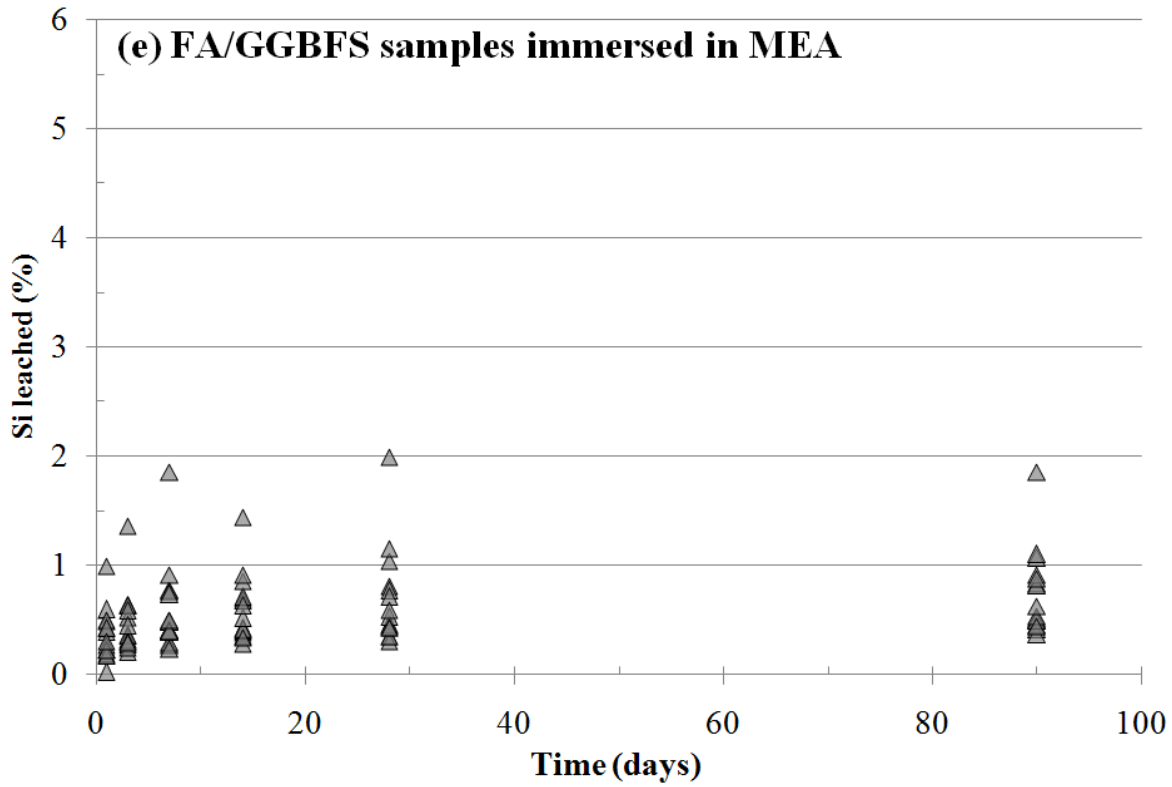
(e) FA/GGBFS samples immersed in MEA
Si leached (%)
Time (days)
0
1
2
3
4
5
6
0
20
40
60
80
100

639

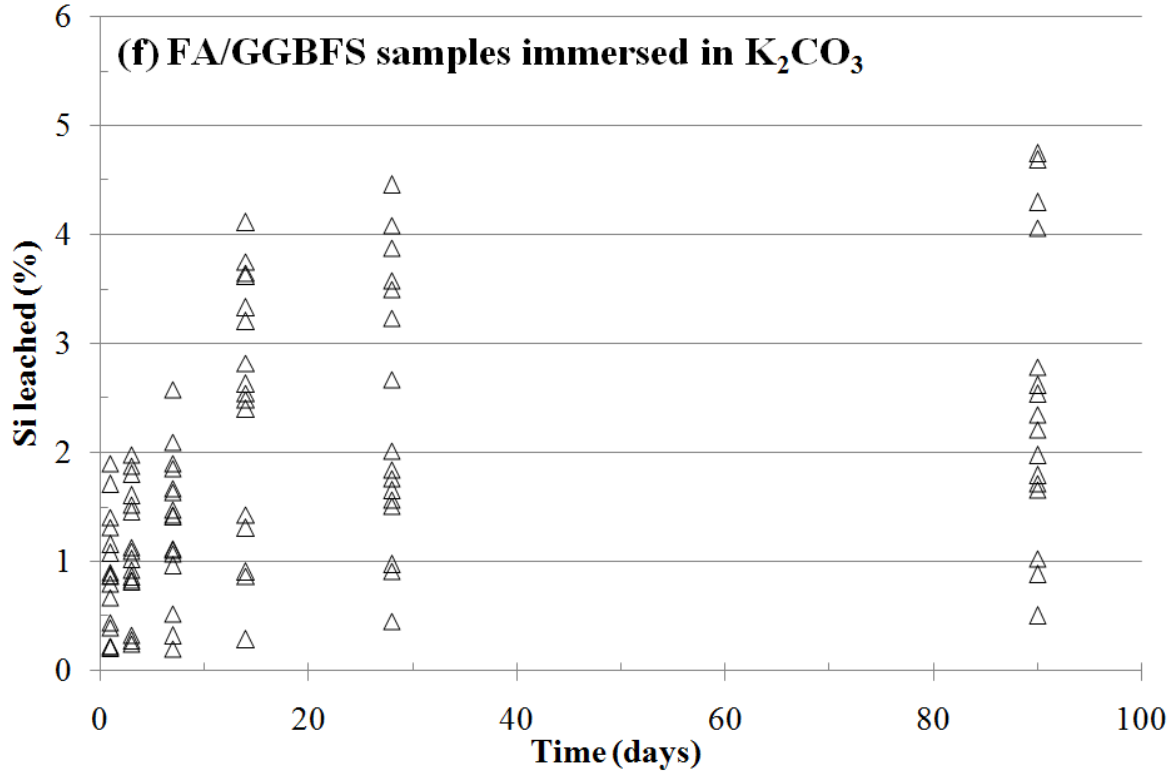
(f) FA/GGBFS samples immersed in K_2CO_3
Si leached (%)
Time (days)
0
1
2
3
4
5
6
0
20
40
60
80
100

640

641 Figure 1. Leaching of Si from (a, b, c) the MK/GGBFS binders and (d, e, f) FA/GGBFS
642 binders during 90 days of solvent exposure, (a, d) H_2O, (b, e) MEA, (c, f) K_2CO_3

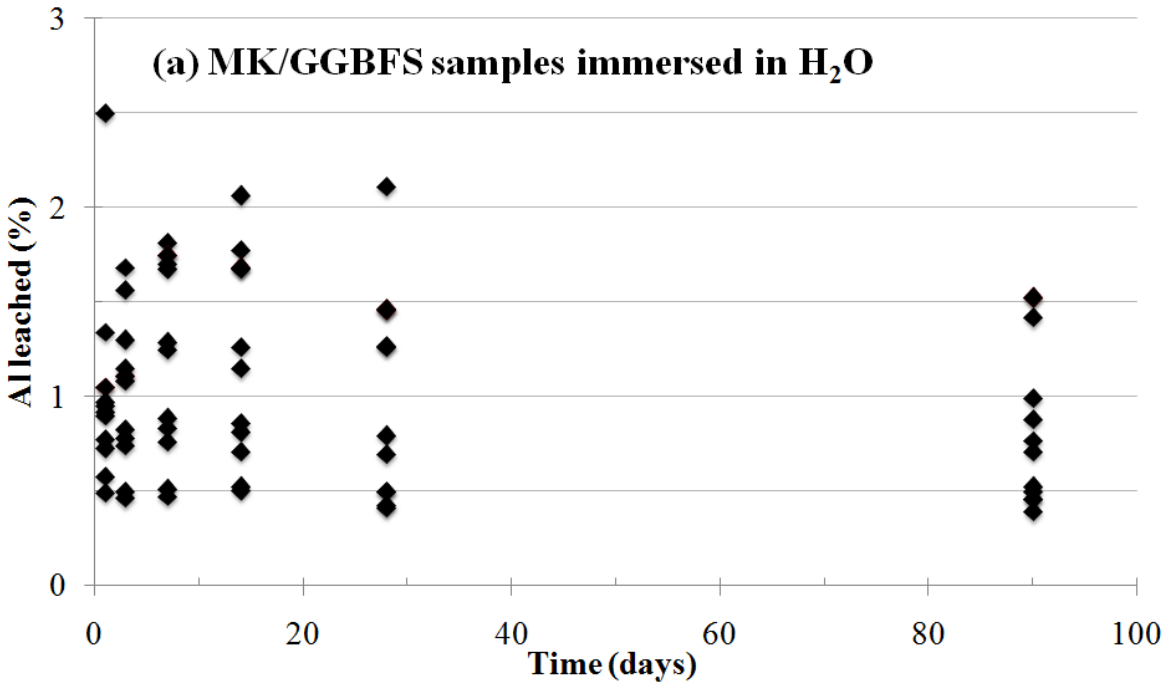

643

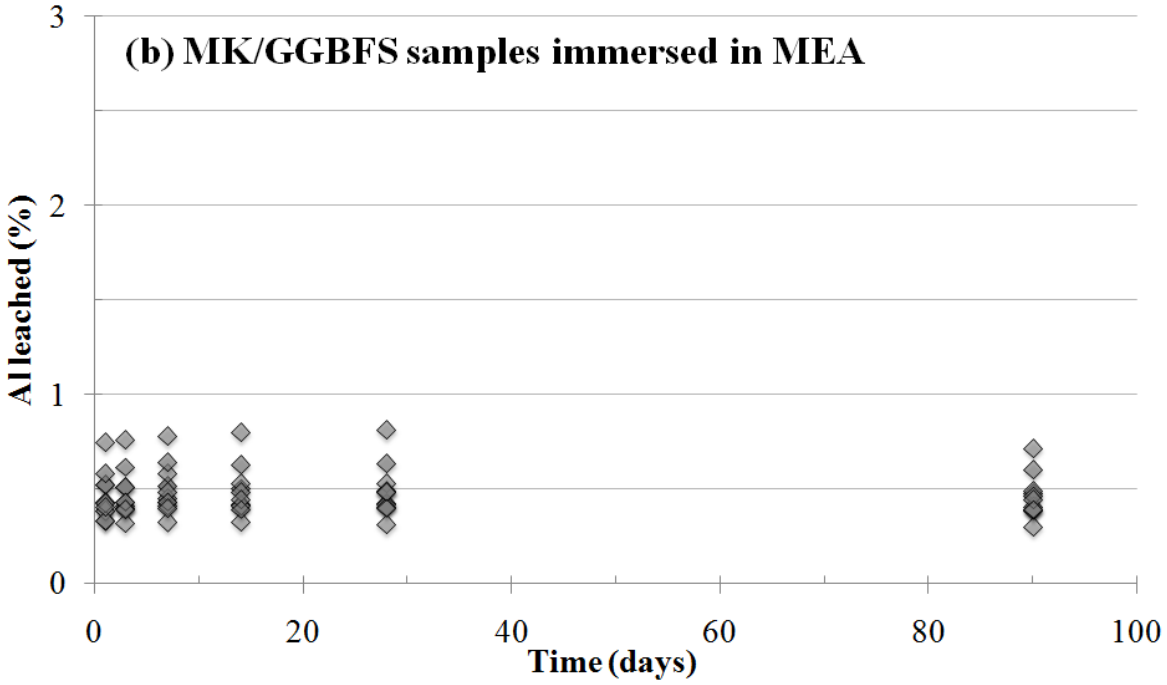

644

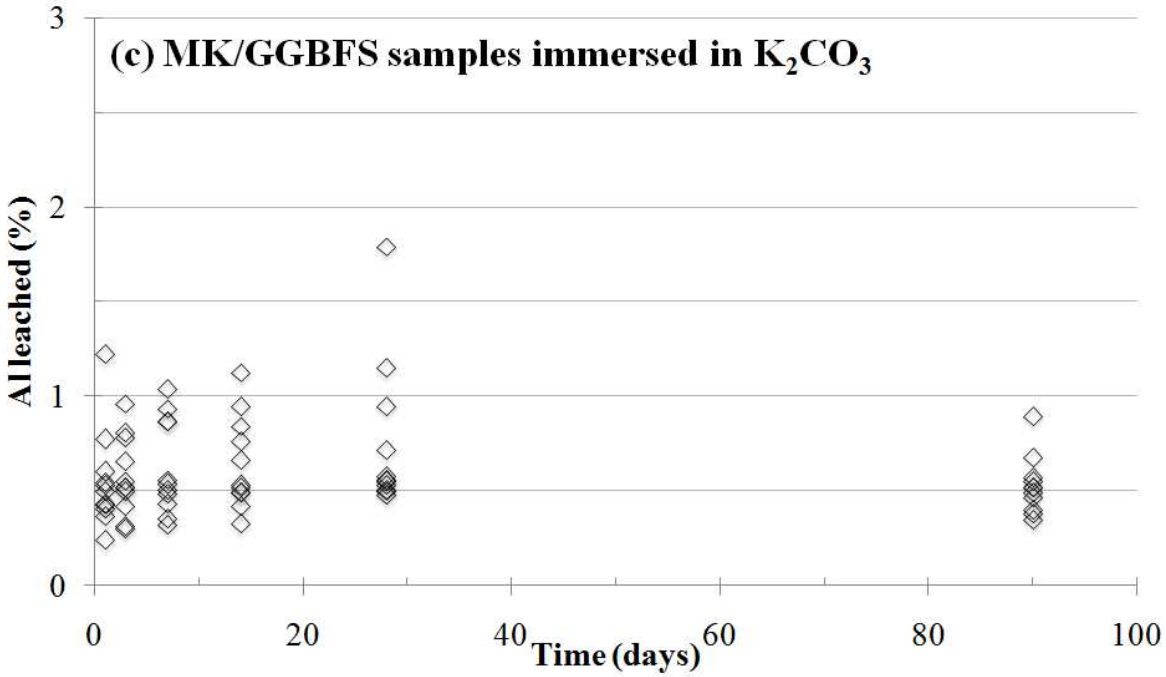
(c) MK/GGBFS samples immersed in K_2CO_3
Al leached (%)
0
1
2
3
0
20
40
60
80
100
Time (days)

645

646

647

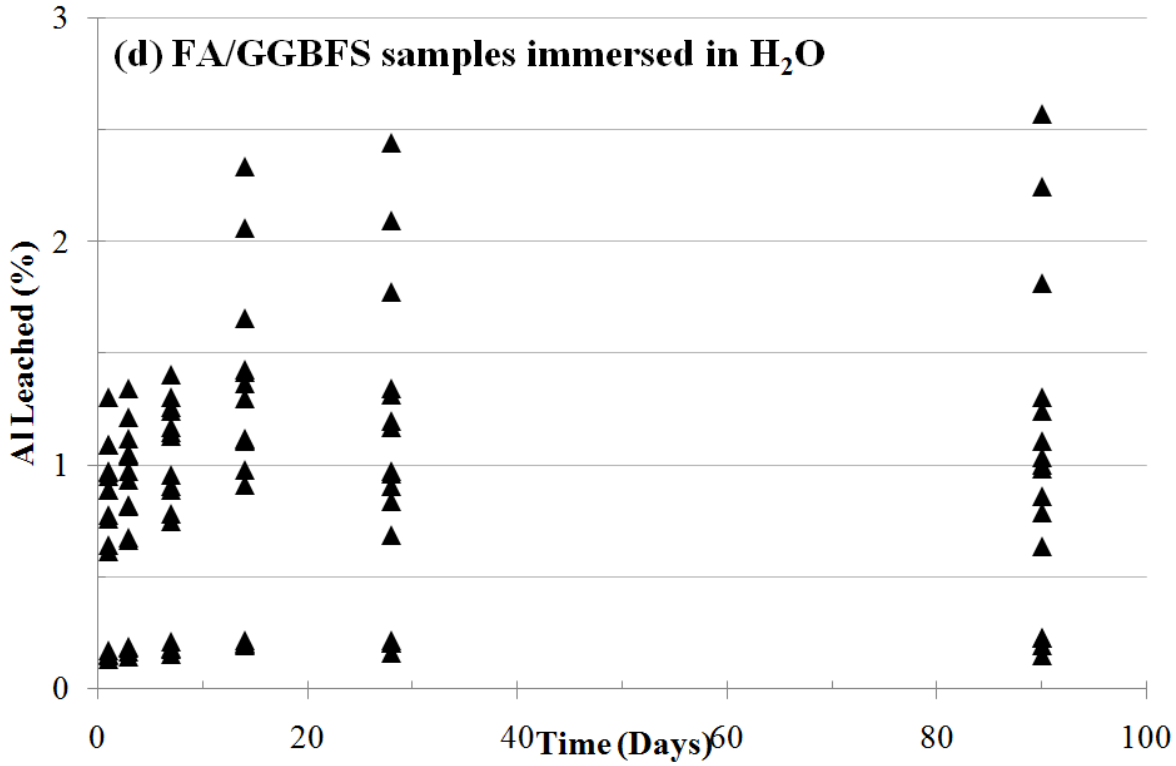
(d) FA/GGBFS samples immersed in H_2O
Al Leached (%)
Time (Days)
0
1
2
3
0
20
40
60
80
100

648

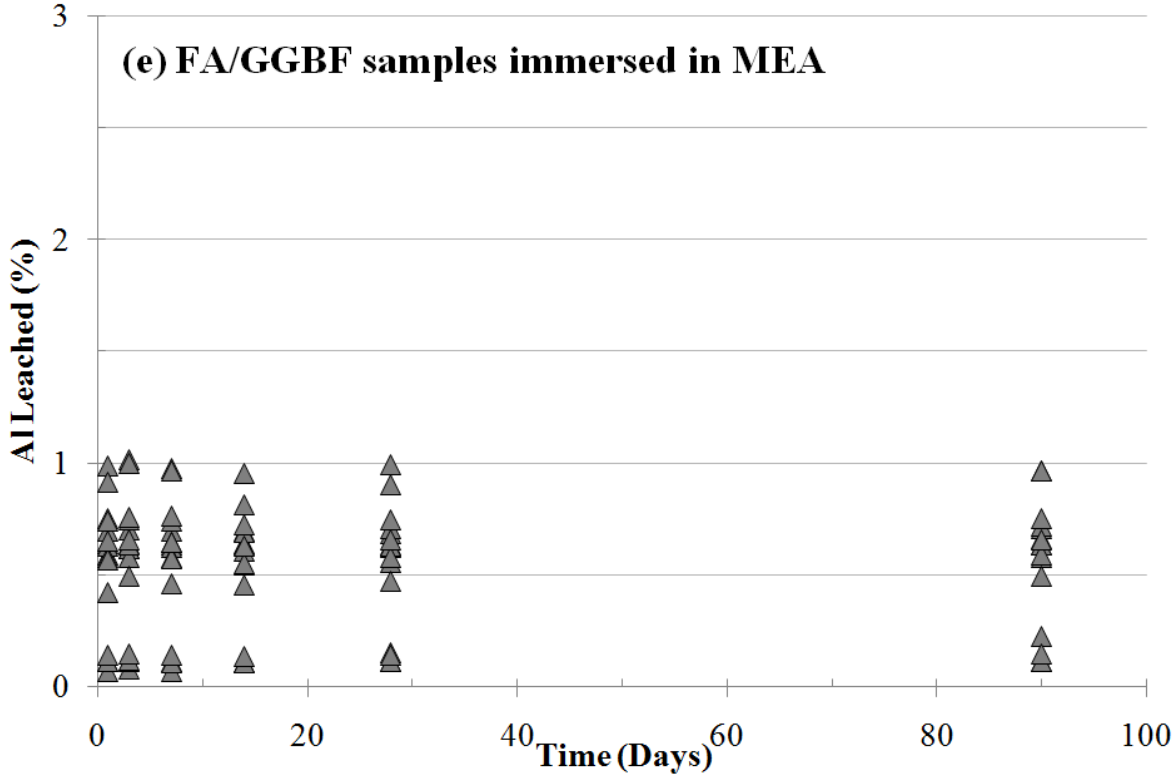
(e) FA/GGBF samples immersed in MEA
Al Leached (%)
Time (Days)
0
1
2
3
0
20
40
60
80
100

649

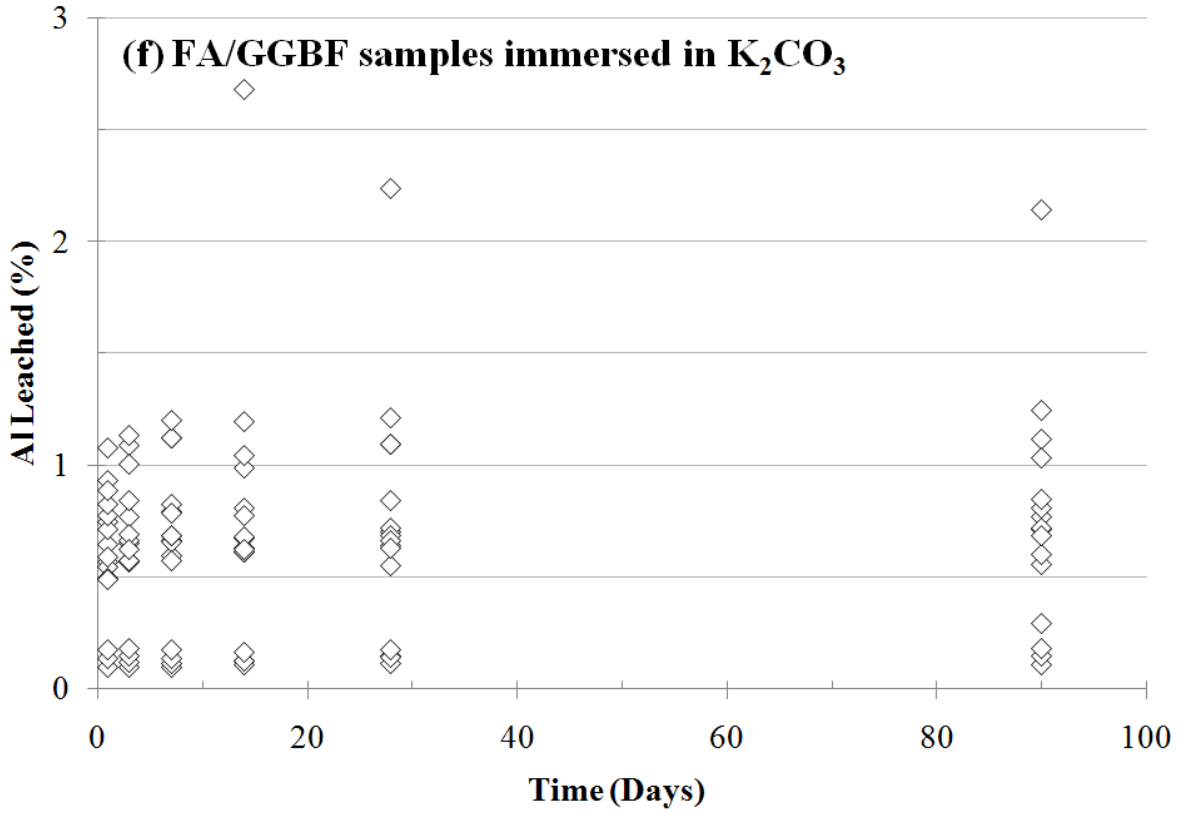

650

651 Figure 2. Leaching of Al from (a, b, c) the MK/GGBFS binders, and (d, e, f) the FA/GGBFS
652 binders during 90 days of solvent exposure, (a, d) H_2O, (b, e) MEA, (c, f) K_2CO_3

653

654

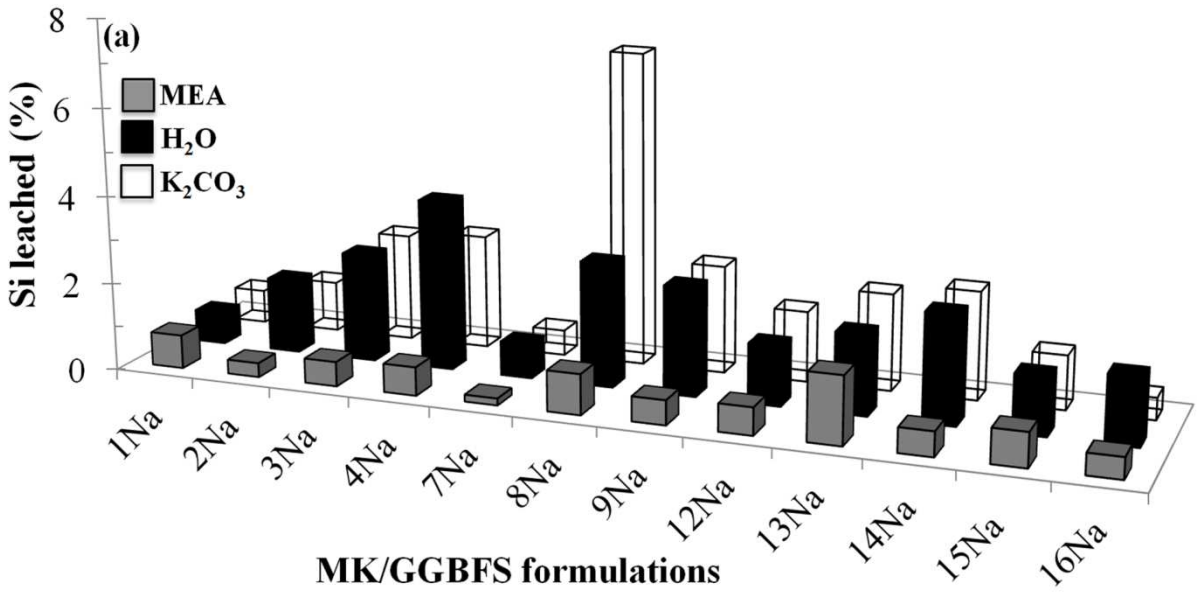

655

656

657

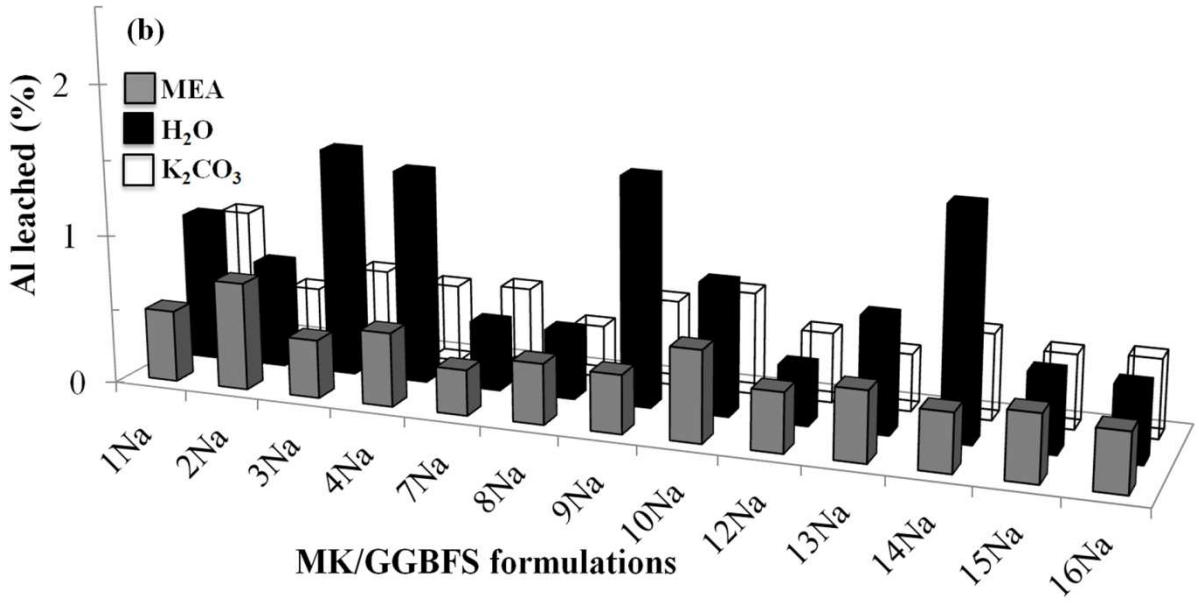

658

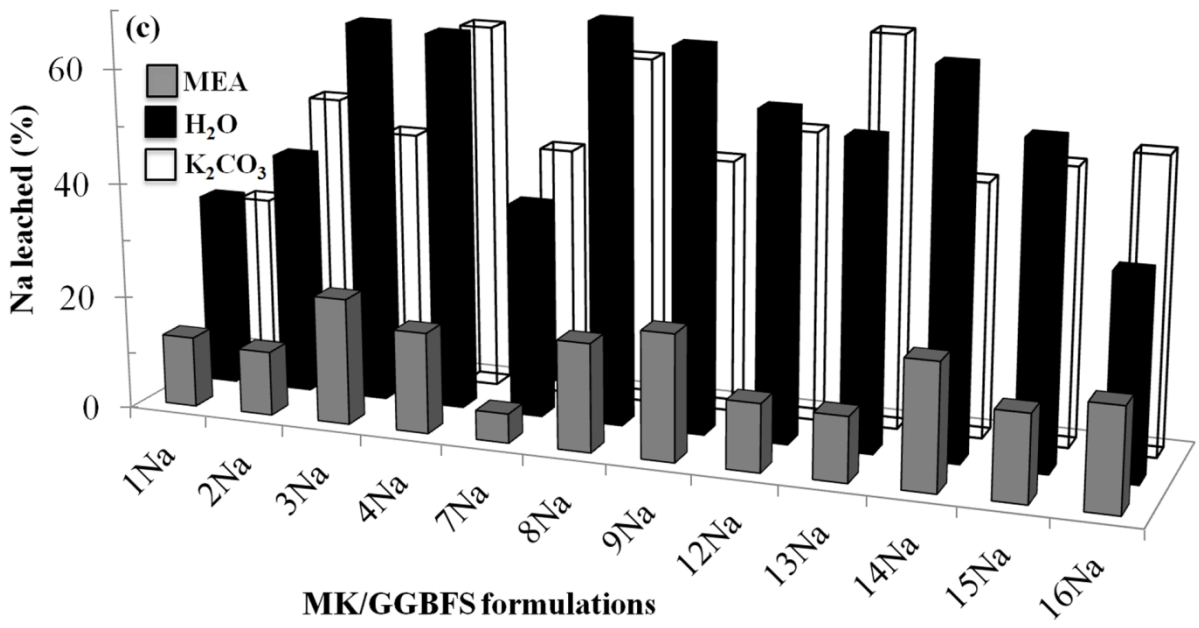
(c)
MEA
H2O
K2CO3
Na leached (%)
0
20
40
60
1Na
2Na
3Na
4Na
7Na
8Na
9Na
12Na
13Na
14Na
15Na
16Na
MK/GGBFS formulations

659

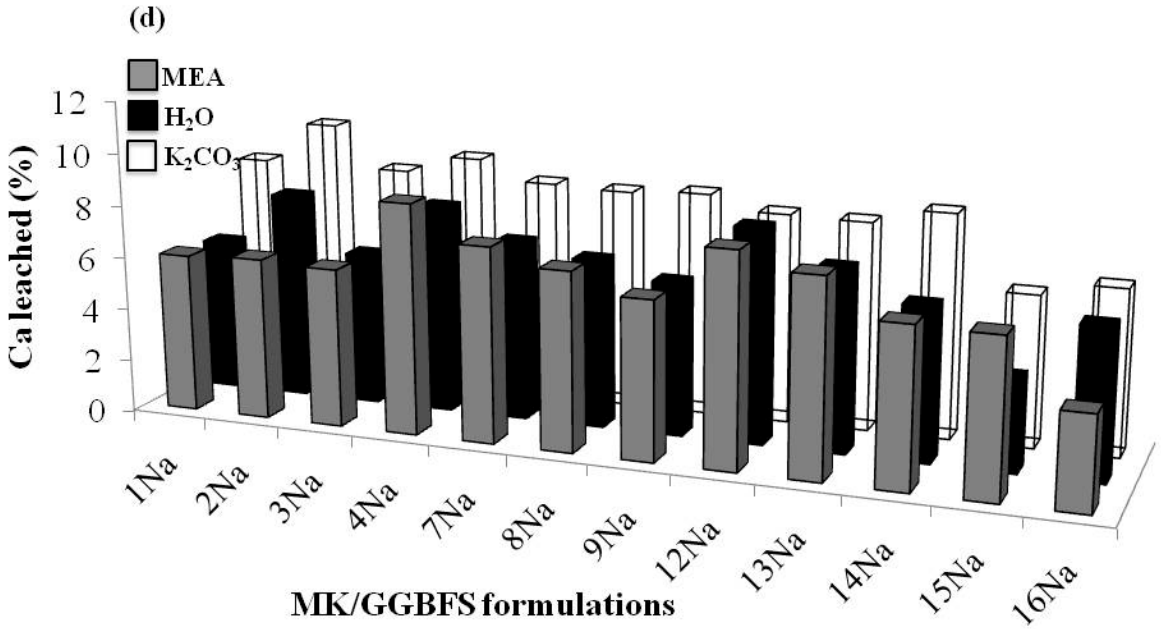
(d)
MEA
H2O
K2CO3
Ca leached (%)
0
2
4
6
8
10
12
1Na
2Na
3Na
4Na
7Na
8Na
9Na
12Na
13Na
14Na
15Na
16Na
MK/GGBFS formulations

660

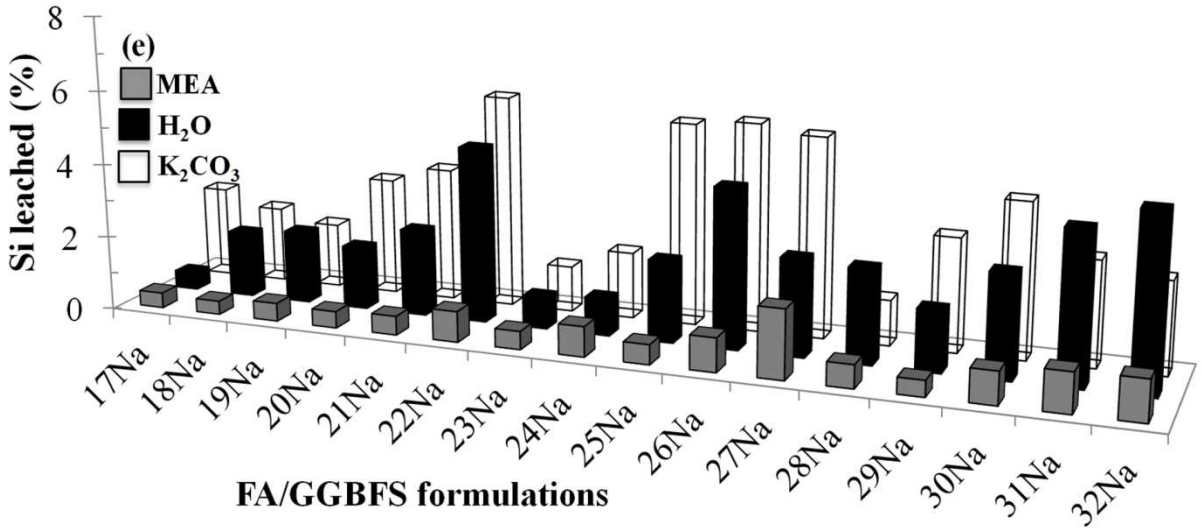
(e)
MEA
H2O
K2CO3
Si leached (%)
0
2
4
6
8
17Na
18Na
19Na
20Na
21Na
22Na
23Na
24Na
25Na
26Na
27Na
28Na
29Na
30Na
31Na
32Na
FA/GGBFS formulations

661

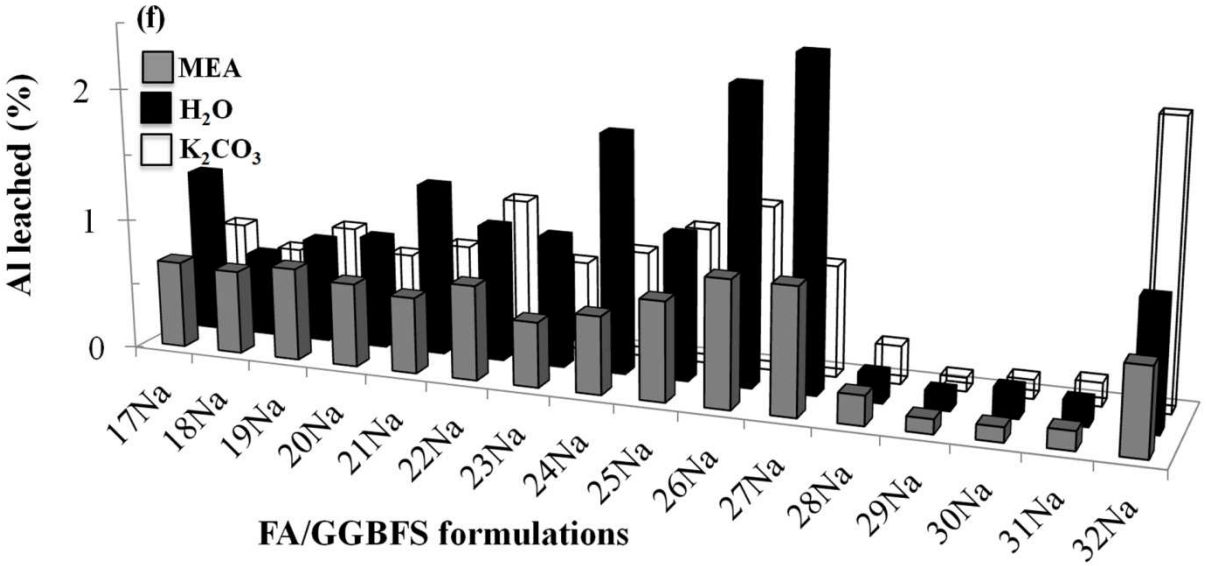
(f)
MEA
H2O
K2CO3
Al leached (%)
0
1
2
17Na
18Na
19Na
20Na
21Na
22Na
23Na
24Na
25Na
26Na
27Na
28Na
29Na
30Na
31Na
32Na
FA/GGBFS formulations

662

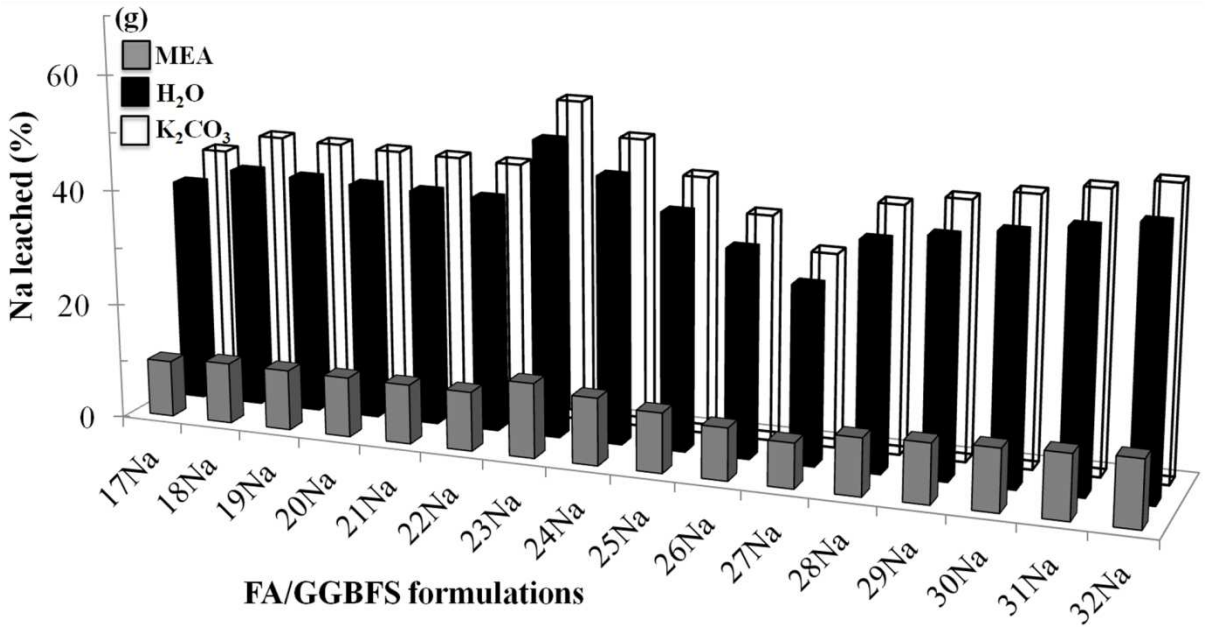

663

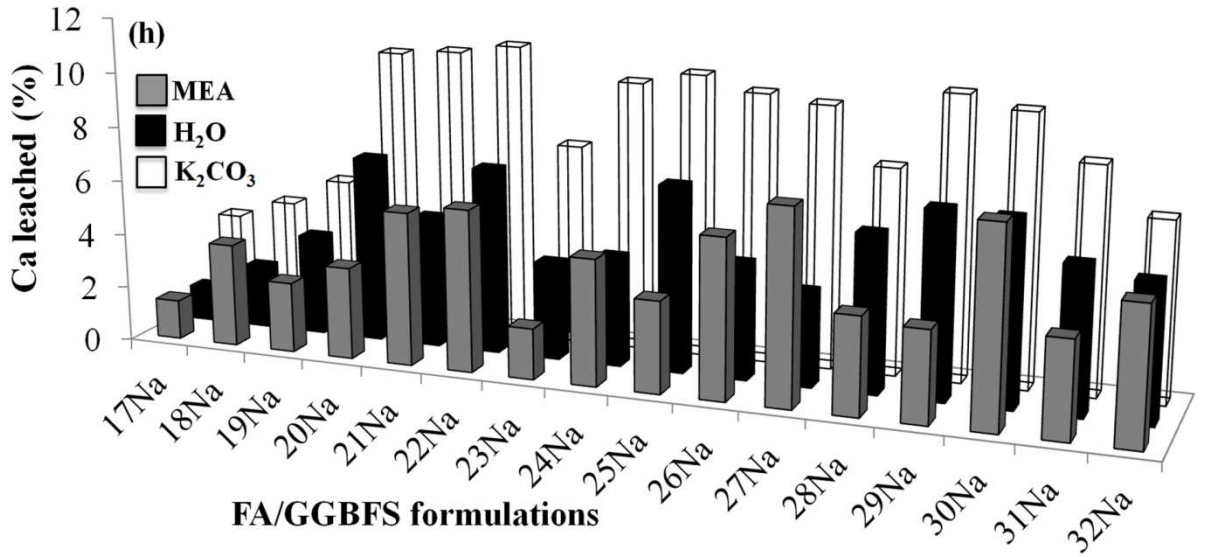

664

665 Figure 3. Leaching of (a) Si (b) Al (c) Na and (d) Ca from each of the MK/GGBFS
666 geopolymer formulations, and of (e) Si, (f) Al, (g) Na and (h) Ca from each of the
667 FA/GGBFS geopolymer formulations, following 90 days of solvent exposure.

668

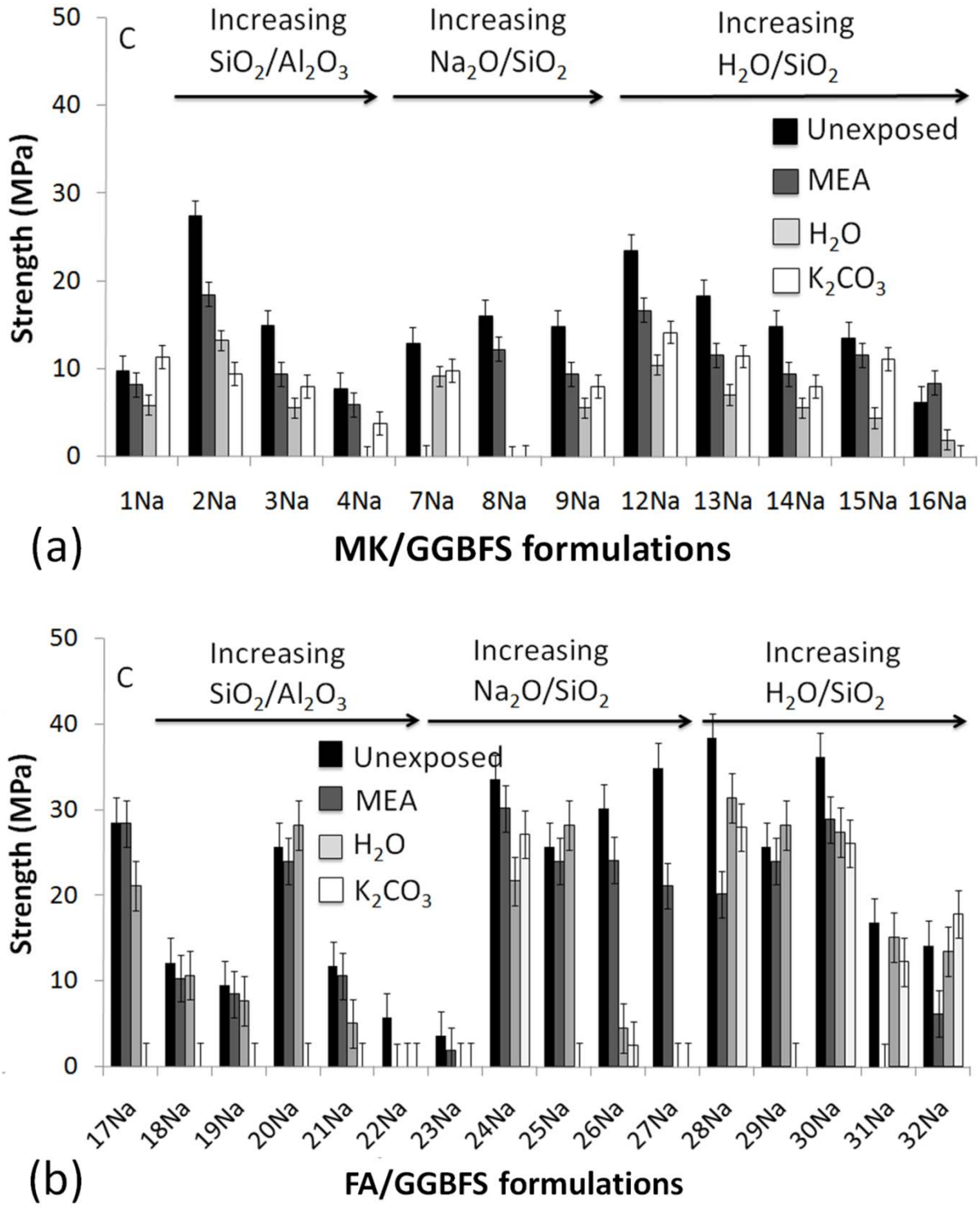

Figure 4. Compressive strengths of the (a) MK/GGBFS and (b) FA/GBFS formulations after 28days of unexposed aging and 28 days of solvent exposure. The formulation trends in each series are marked with arrows, and c denotes the control sample (without GGBFS) in each set.

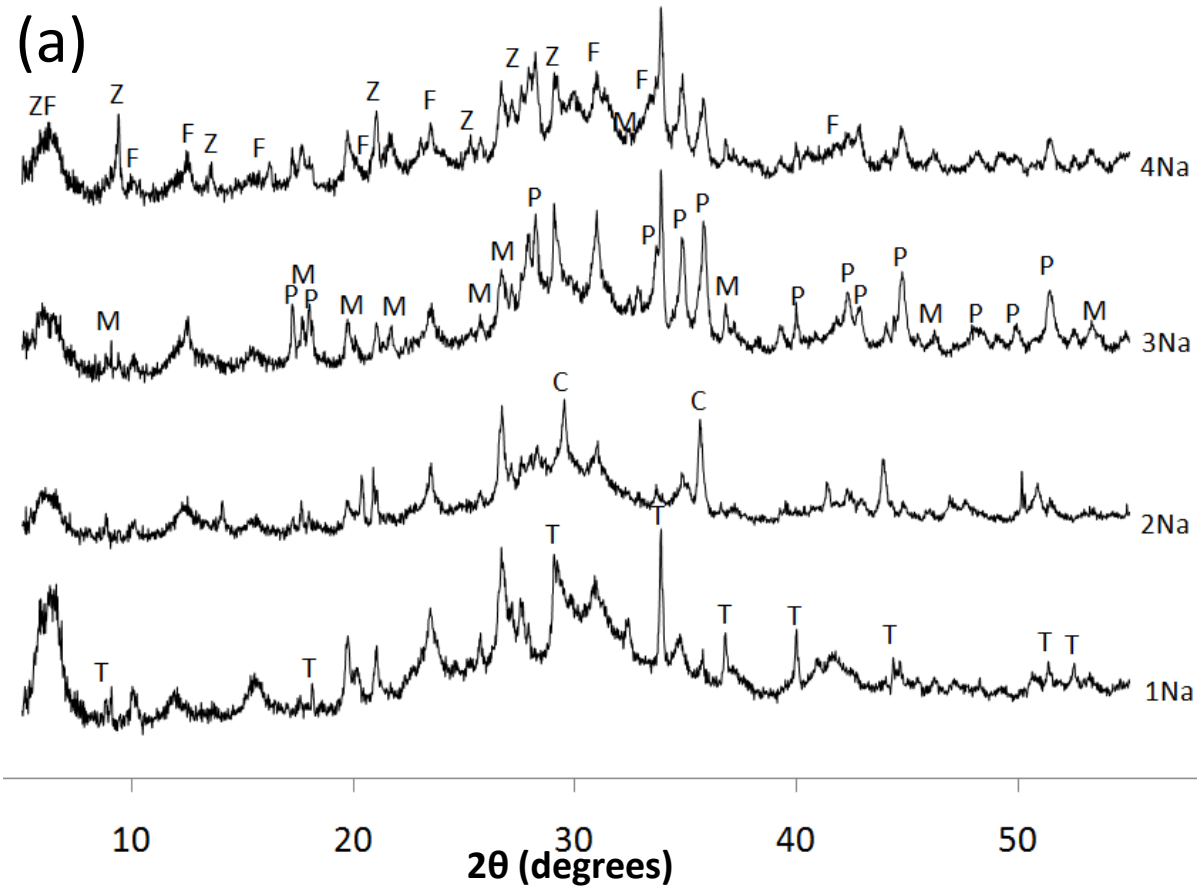

677
678

679

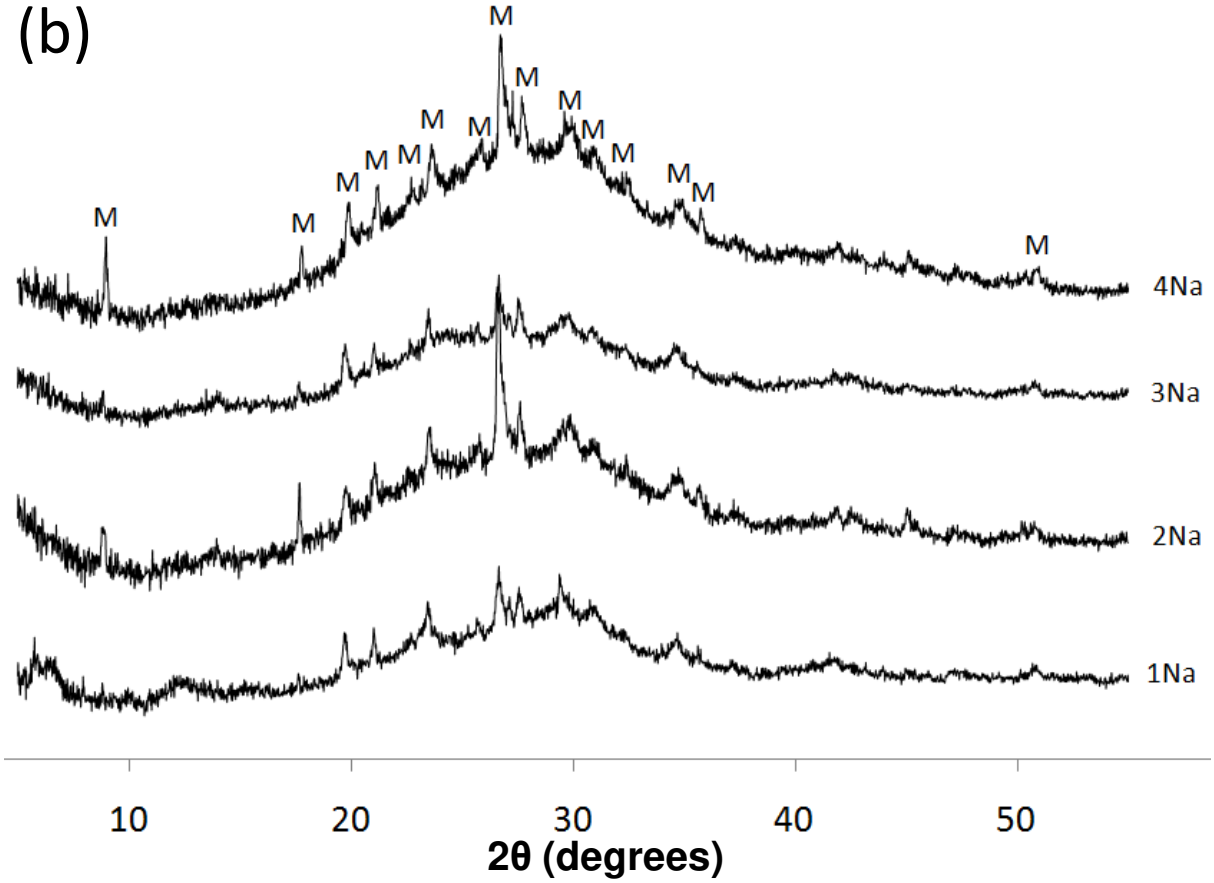

680
681

682

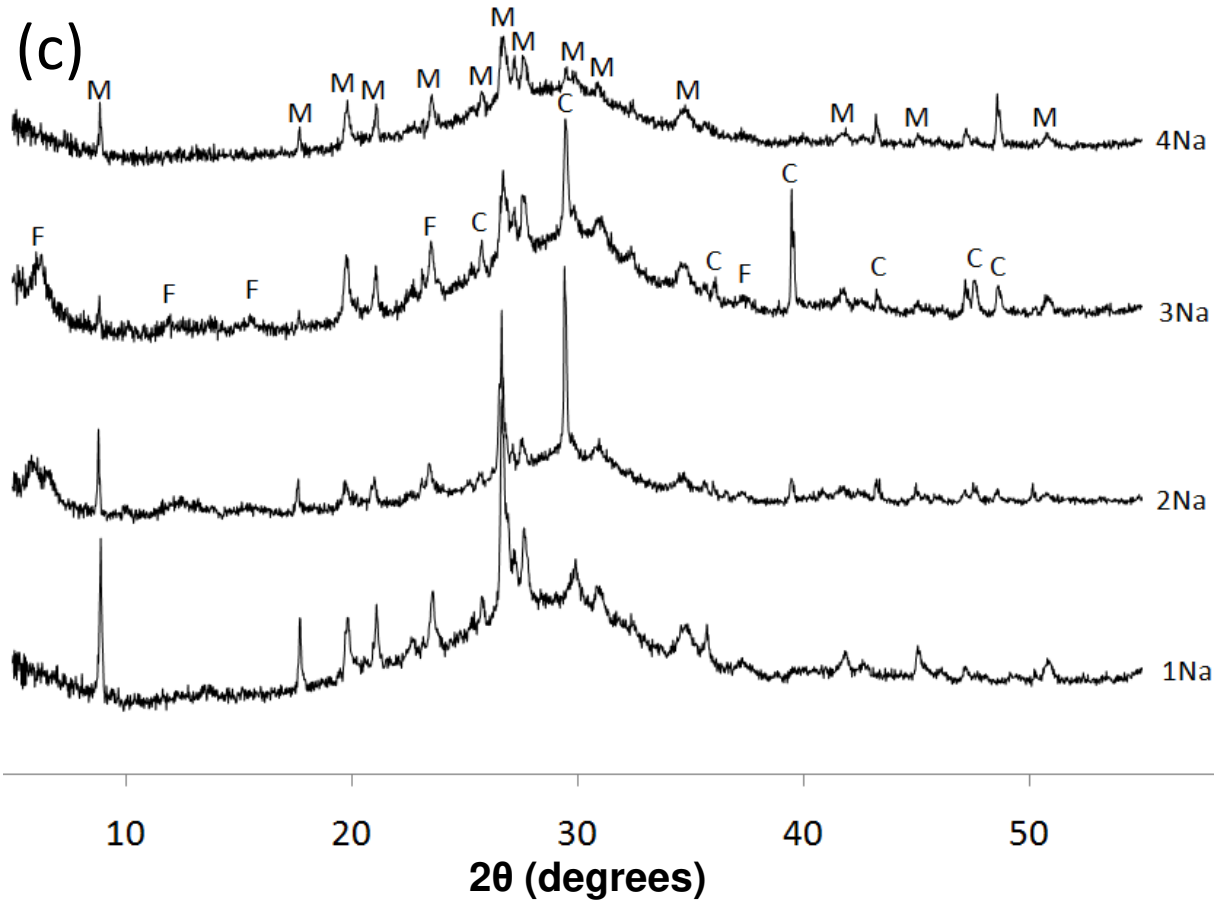
(c)
M
M
M
M
M
M
M
M
M
M
M
M
M
C
M
M
M
4Na
F
F
F
F
C
C
C
F
C
C
C
3Na
2Na
1Na
10
20
30
40
50
2θ (degrees)

683
684

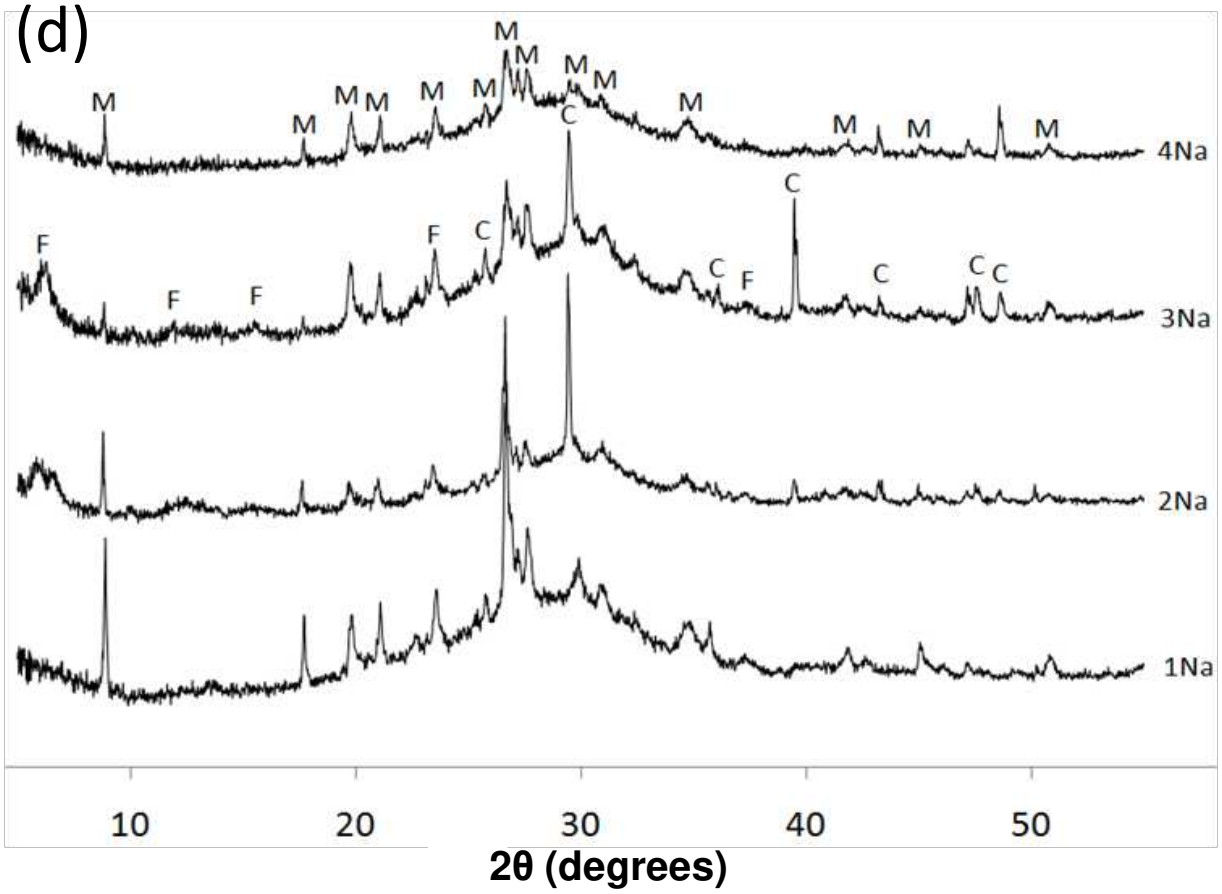

685
686

687 Figure 5. XRD traces of MK/GGBFS samples 1Na-4Na after (a) 7 days of curing and 90 days
688 of aging, or 7 days of curing and 90 days of exposure to solvents: (b) MEA; (c) Milli-Q H_2O;
689 (d) K_2CO_3. Phases marked are C: calcite, F: faujasite, M: muscovite, P: pirssonite, T: trona,
690 Z: chabazite-Na.

691

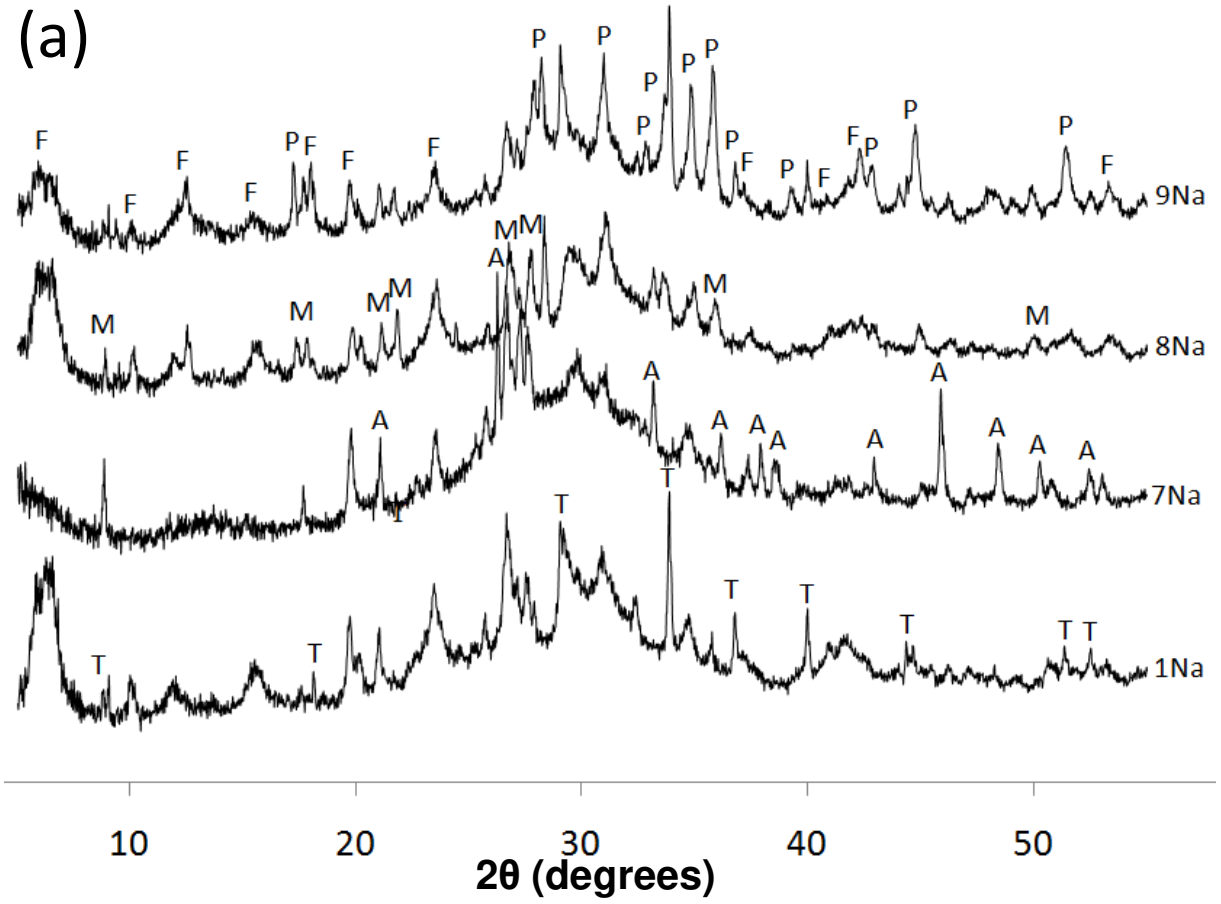

692
693

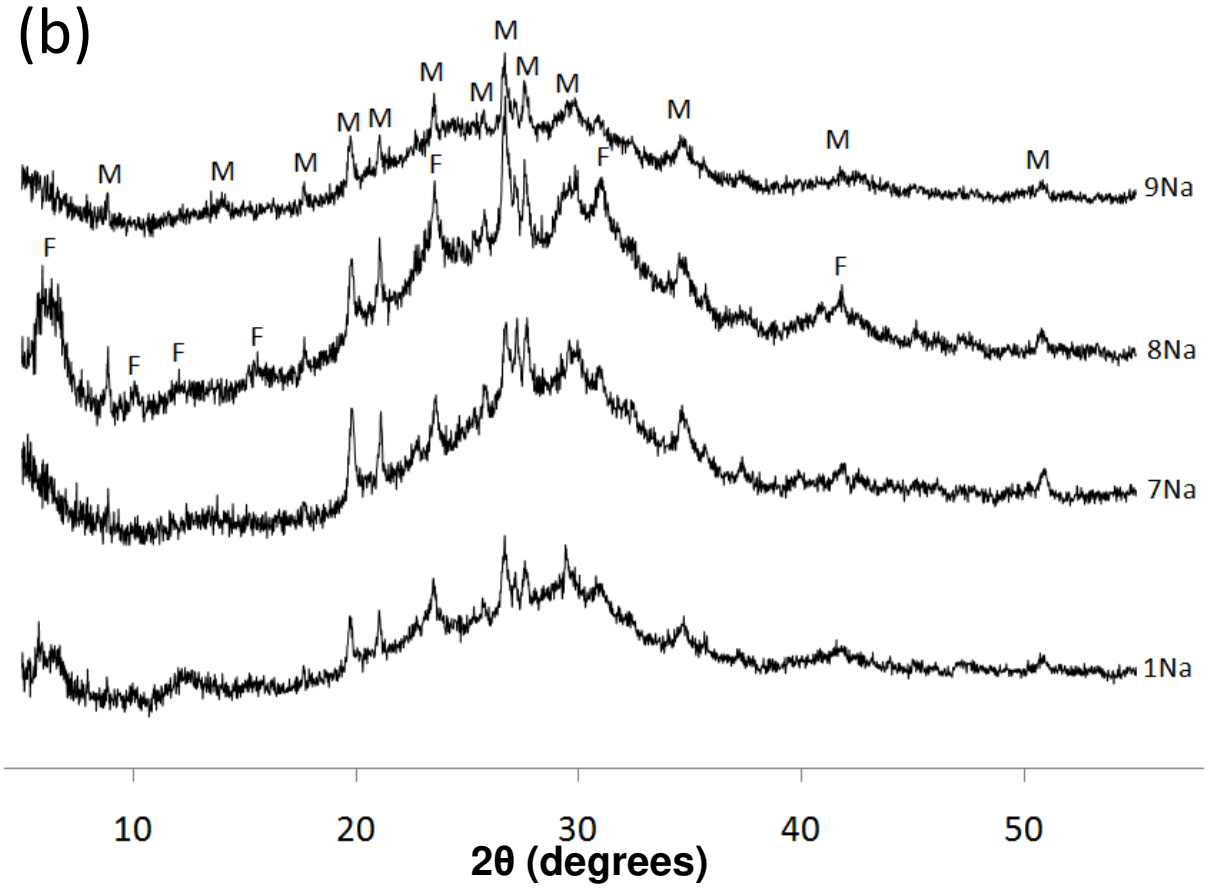
(b)
M
M
M
M
M
M
M
M
M
M
M
M
M
F
F
F
F
F
F
F
F
9Na
8Na
7Na
1Na
10
20
30
40
50
2θ (degrees)

694
695

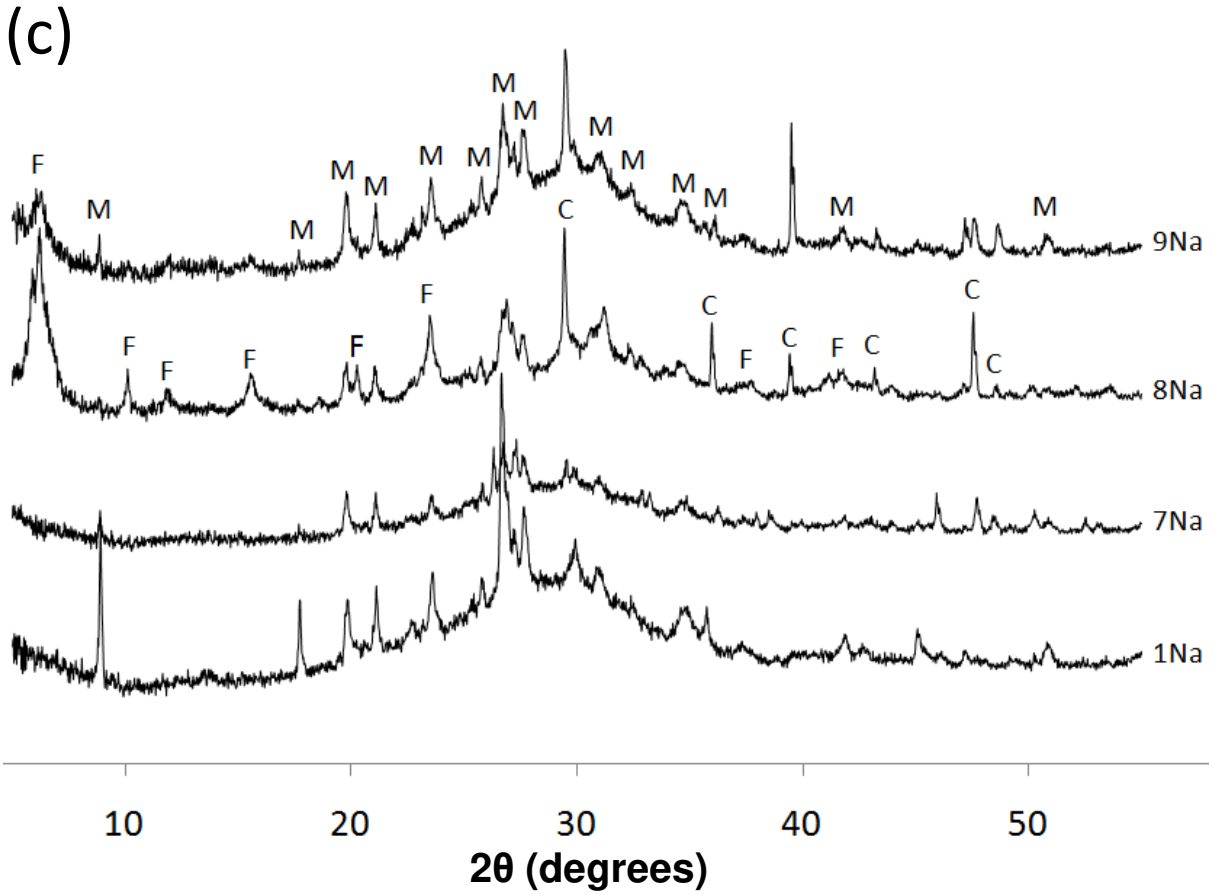
(c)
F
M
M
M
M
M
M
M
M
M
M
M
M
M
M
C
9Na
F
F
F
F
F
C
C
F
C
F
C
C
C
8Na
7Na
1Na
10
20
30
40
50
2θ (degrees)

696
697

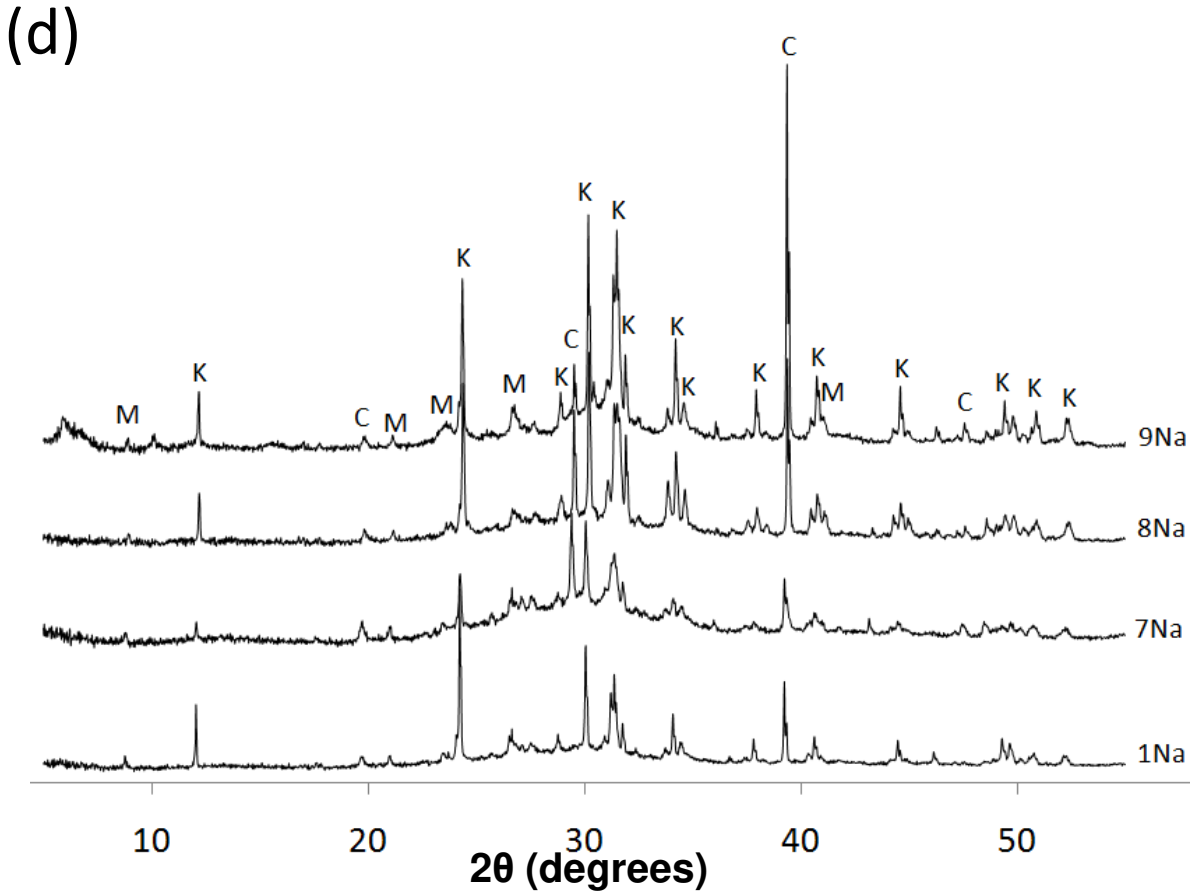

698
699

700 Figure 6. XRD traces of MK/GGBFS samples 1Na and 7Na-9Na after (a) 7 days of curing
701 and 90 days of aging, or 7 days of curing and 90 days of exposure to solvents: (b) MEA; (c)
702 Milli-Q H_2O; (d) K_2CO_3. Phases marked are A: aragonite, C: calcite, F: faujasite, K:
703 kalcinite, M: muscovite, P: pirssonite, T: trona, Z: chabazite-Na.

704

705

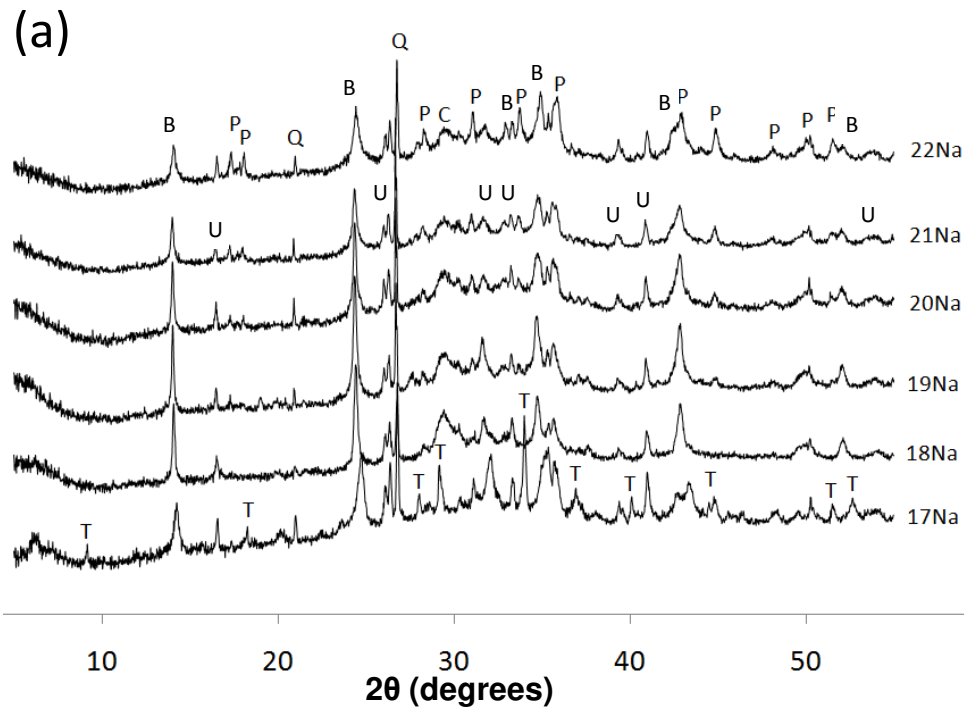
(a)
22Na
21Na
20Na
19Na
18Na
17Na
10
20
30
40
50
2θ (degrees)

706

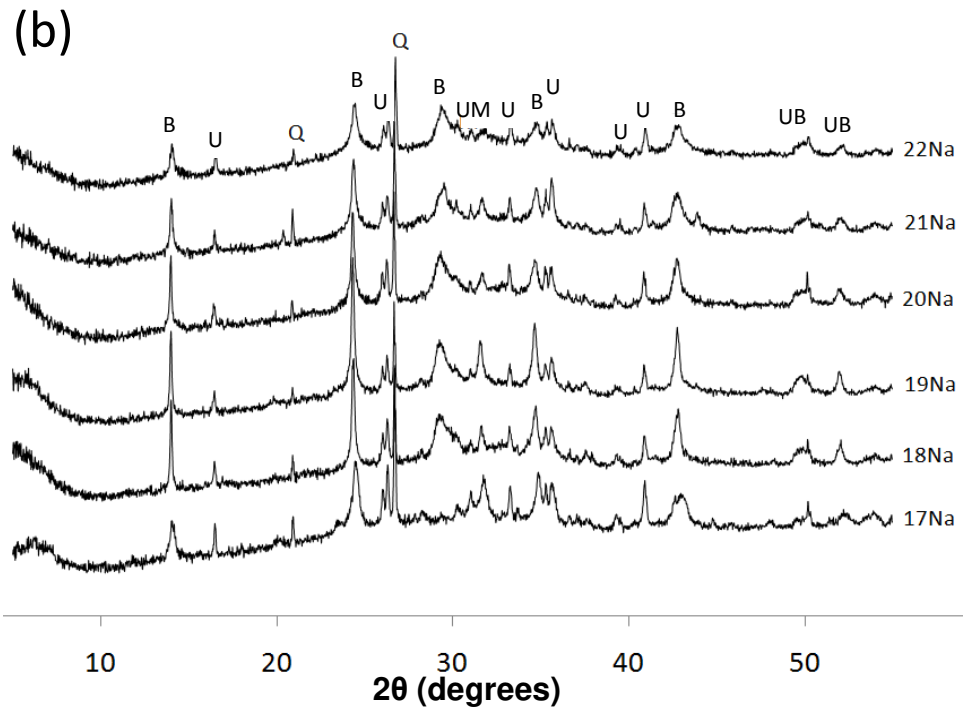
(b)
22Na
21Na
20Na
19Na
18Na
17Na
10
20
30
40
50
2θ (degrees)

707

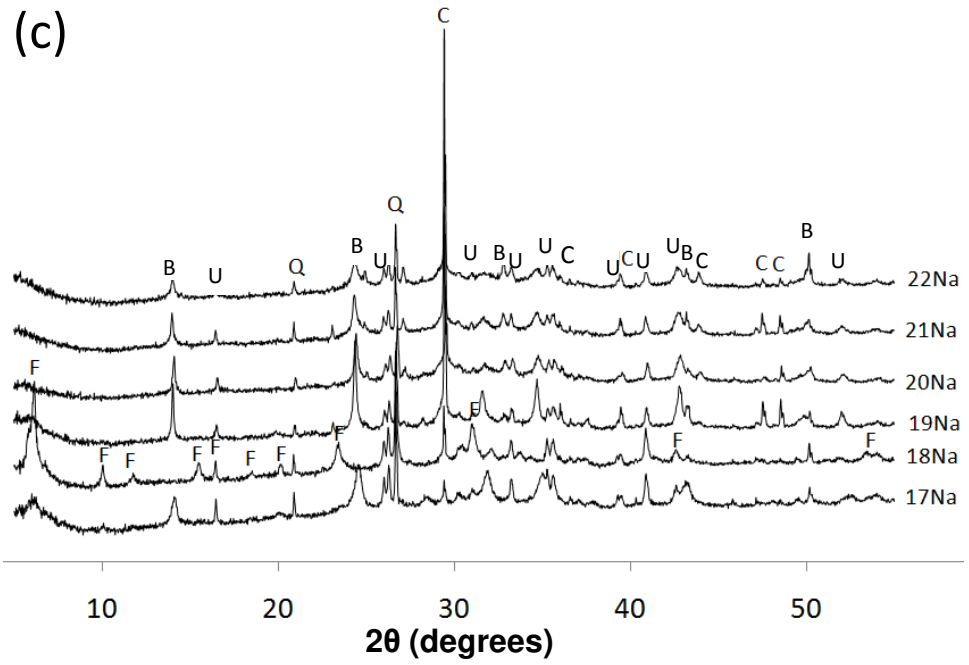

708

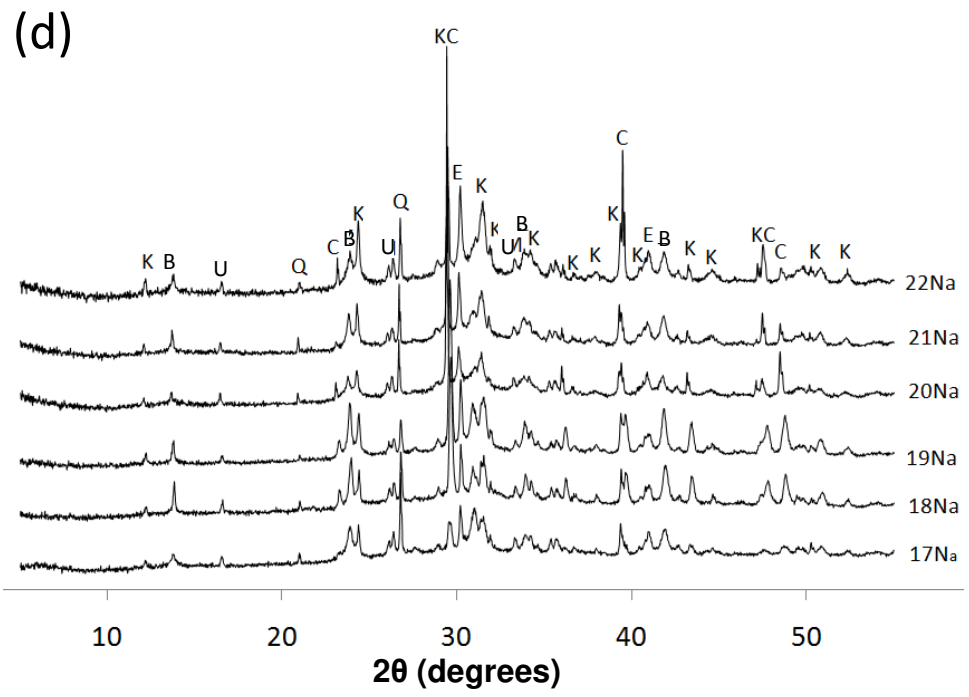

709

710 Figure 7. XRD traces of FA/GGBFS samples 17Na-22Na after (a) 7 days of curing and 90
711 days of aging, or 7 days of curing and 90 days of exposure to solvents: (b) MEA; (c) Milli-Q
712 H_2O; (d) K_2CO_3. Phases marked are B: basic sodalite, U: mullite, Q: quartz, P: pirssonite, C:
713 calcite, T: trona, F: faujasite, K: kalcinite, E: potassium carbonate.

714

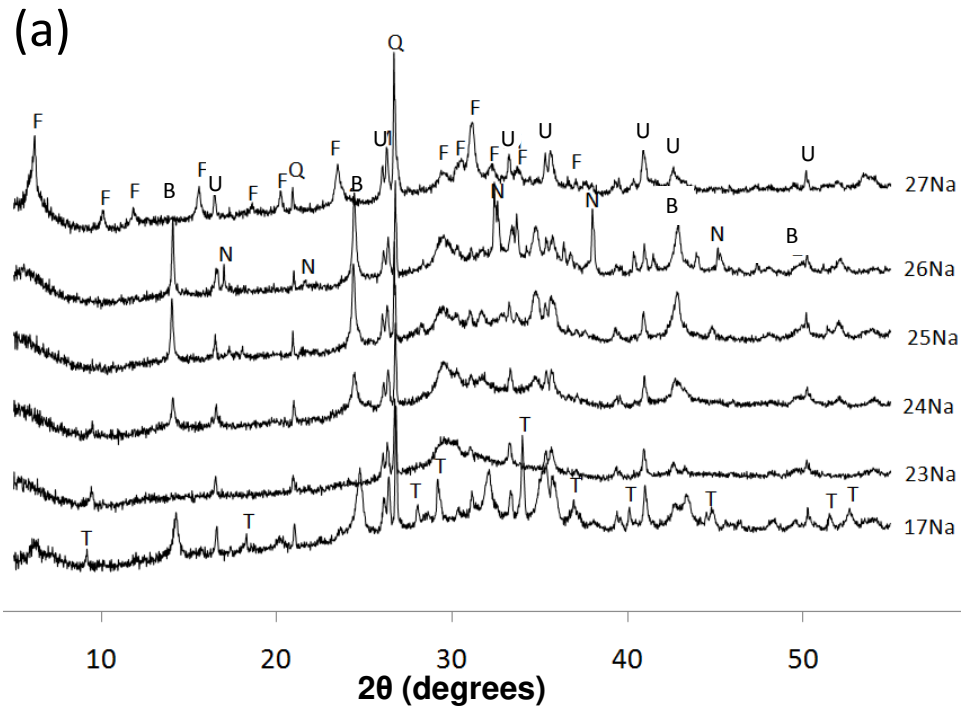
(a)
Q
F
U
B
N
T
27Na
26Na
25Na
24Na
23Na
17Na
10
20
30
40
50
2θ (degrees)

715

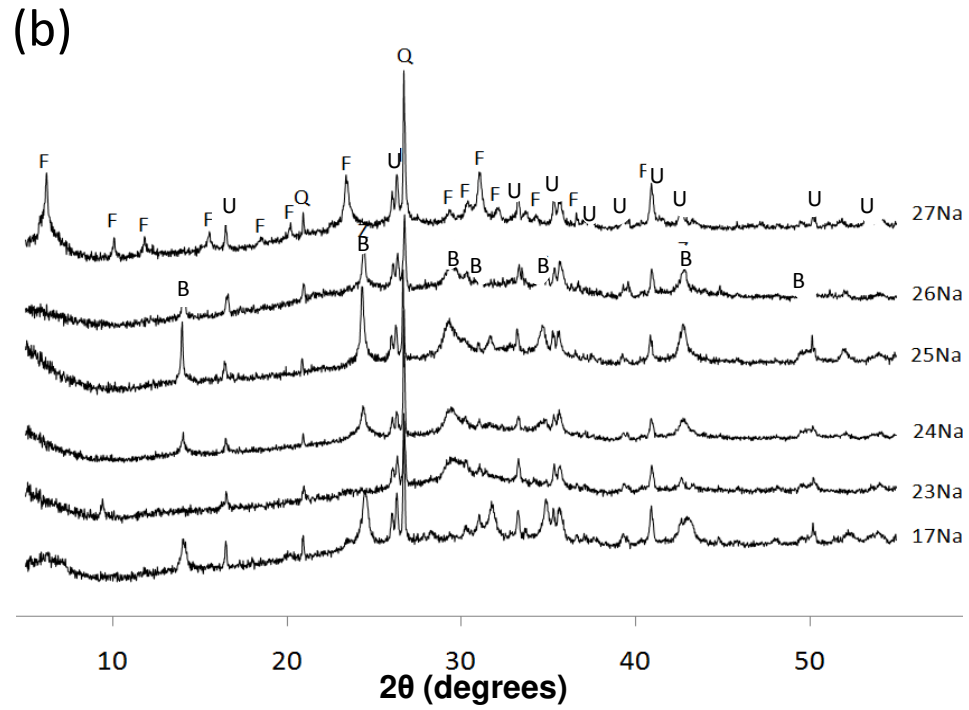
(b)
Q
F
U
B
27Na
26Na
25Na
24Na
23Na
17Na
10
20
30
40
50
2θ (degrees)

716

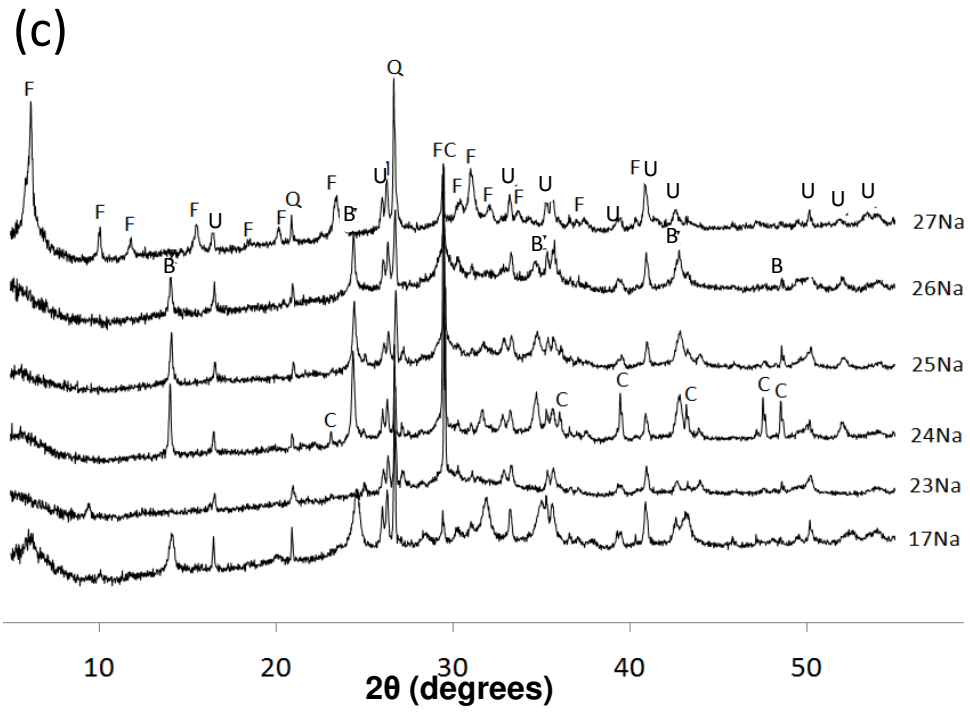

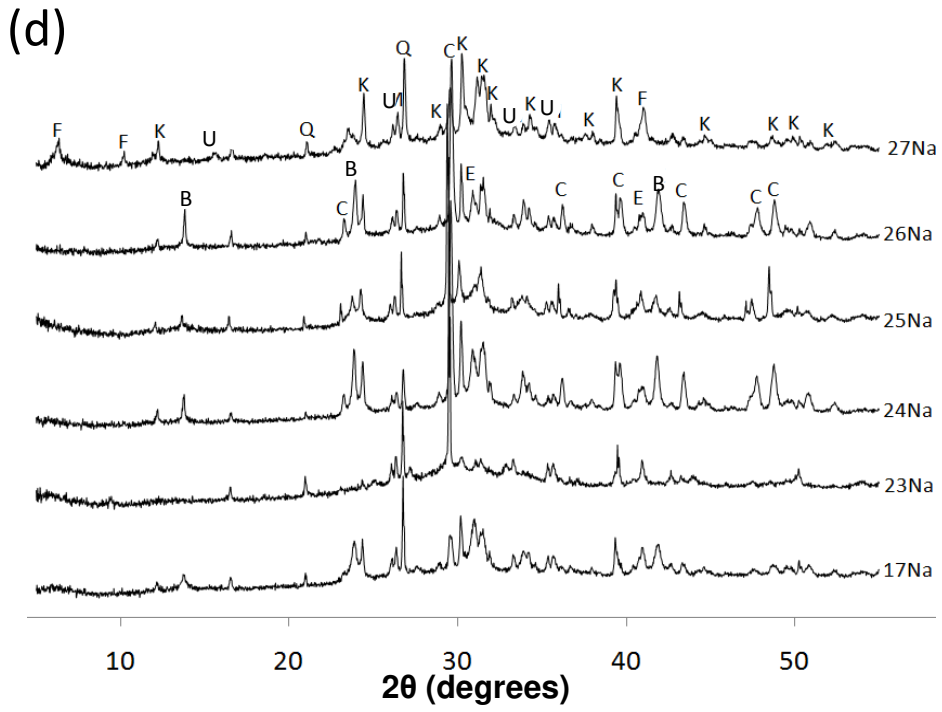

Figure 8. XRD traces of FA/GGBFS samples 17Na and 23Na-27Na after (a) 7 days of curing and 90 days of aging, or 7 days of curing and 90 days of exposure to solvents: (b) MEA; (c) Milli-Q H_2O; (d) K_2CO_3. Phases marked are B: basic sodalite, F: faujasite, Q: quartz, U: mullite, N: thermonatrite, T: trona, C: calcite, K: kalcinite, E: potassium carbonate.